Received: 6 April 2022 | Revised: 13 June 2022 | Accepted: 22 June 2022

DOI: 10.1002/jmor.21494

RESEARCH ARTICLE

JOURNAL OF morphology WILEY

Morphology of ctenostome bryozoans: 5. *Sundanella*, with description of a new species from the Western Atlantic and the Multiporata concept

Thomas Schwaha[1] | Judith E. Winston[2] | Dennis P. Gordon[3]

[1]Department of Evolutionary Biology, University of Vienna, Vienna, Austria

[2]Smithsonian Marine Station, Fort Pierce, Florida, USA

[3]National Institute of Water and Atmospheric Research (NIWA), Wellington, New Zealand

Correspondence
Thomas Schwaha, Department of Evolutionary Biology, University of Vienna, Schlachthausgasse 43, 1030 Vienna, Austria.
Email: thomas.schwaha@univie.ac.at

Abstract

Ctenostome bryozoans are a small group of gymnolaemates that comprise only a few hundred described species. Soft-tissue morphology remains the most important source for analysing morphological characters and inferring relationships within this clade. The current study focuses on the genus *Sundanella*, for which morphological data is scarce to almost absent. We studied two species of the genus, including one new to science, using histology and three-dimensional reconstruction techniques and confocal laser scanning microscopy. *Sundanella* generally has a thick, sometimes arborescent cuticle and multiporous interzooidal pore plates. The lophophore is bilateral with an oral rejection tract and generally has 30 or 31 tentacles in both species. The digestive tract shows a large cardia in *S. floridensis* sp. nov. and an extremely elongated intestine in *Sundanella sibogae*. Both terminate via a vestibular anus. Only parietodiaphragmatic muscles are present and four to six duplicature bands. Both species show a large broad frontal duplicature band further splitting into four individual bands. The collar is vestibular. *Sundanella sibogae* shows highly vacuolated cells at the diaphragm, whereas *S. floridensis* sp. nov. has unique glandular pouches at the diaphragmal area of the tentacle sheath. Such apertural glands have never been encountered in other ctenostomes. Both species of *Sundanella* are brooders that brood embryos either in the vestibular or cystid wall. Taken together, the current analysis shows numerous characteristics that refute an assignment of *Sundanella* to victorellid ctenostomes, which only show superficial resemblance, but differ substantially in most of their soft-body morphological traits. Instead, a close relationship with other multiporate ctenostomes is evident and the families Pherusellidae, Flustrellidrae and Sundanellidae should be summarized as clade 'Multiporata' in the future.

KEYWORDS

ctenostome evolution, Gymnolaemata, apertural glands, *Sundanella floridensis* sp. nov.

1 | INTRODUCTION

Bryozoa is a phylum of lophotrochozoans characterized by small zooids that typically bud new zooids asexually to form colonies of various shapes and sizes. Zooids comprise an outer body wall (cystid) and internal soft tissues (polypide). The latter mainly consists of the ciliated tentacle crown or lophophore, which the animals use for suspension-feeding, the digestive tract and associated neural and muscular tissue and also gonads (Mukai et al., 1997). Typical for all bryozoans is a defensive response that retracts the polypide into the cystid via prominent retractor muscles (Ryland, 1970).

Systematists divide bryozoans into two clades, Phylactolaemata and Myolaemata. The latter represents the large bulk of bryozoans and contains the Stenolaemata (with the only recent taxon Cyclostomata) and the Gymnolaemata, which comprises the ctenostomes and the Cheilostomata (Schwaha, Ostrovsky, et al., 2020). Ctenostome bryozoans are a small clade of little-studied bryozoans with only about 350 species described (Schwaha, 2020a). In addition, they are paraphyletic and ctenostome-grade/-like forms that were ancestral to the Cheilostomata (Taylor & Waeschenbach, 2015; Todd, 2000). However, it remains unknown which of the recent ctenostome taxa represents the most closely related clade to Cheilostomata.

In the last years, a series of morphological studies on ctenostome bryozoans was undertaken to provide detailed morphological accounts of these little-known forms for further comparative and systematic analyses (Schwaha, 2021; Schwaha & De Blauwe, 2020; Schwaha et al., 2021; Schwaha, Grischenko, et al., 2020). Particularly because cystid characters show high variability in bryozoans (e.g., Jebram, 1982; Waeschenbach et al., 2009), soft-tissue morphology adds substantial depth to our understanding of these bryozoans (see also Schwaha, Ostrovsky, et al., 2020).

Sundanella is an interesting ctenostome genus, erected in 1939 by Braem for a southeast Asian species originally assigned to the genus *Victorella* (Harmer, 1915), but later reassigned owing to several morphological characters (see Braem, 1939). The type material of *S. sibogae* was dredged from areas close to the Indonesian islands of Sulawesi and Tanah Jampea (Harmer, 1915). *Sundanella sibogae* has also been reported from many warm water localities around the world besides Indonesia, including Africa from the Cape Verde Islands to Angola (Cook, 1968, 1985). Subsequently, a few studies were conducted on *Sundanella* material from North Carolina to Florida on the Southern USA East Coast and the Caribbean in the Western Atlantic (Maturo, 1957; Osburn, 1940; Santagata, 2008; Shier, 1964; Winston, 1982) and the Southwestern Atlantic coast in Brazil (Marcus, 1937, 1941). More recently, the newly collected material of the latter was identified as a new species and described as *Sundanella rosea* (Vieira et al., 2014). The species name of *S. rosea* refers to the colour of brooded embryos, a feature which in ctenostomes is known to vary depending on nutrition (cf. Jebram, 1982).

The genus *Sundanella* was originally assigned to the victorelloidean ctenostomes—a non-monophyletic group of ctenostomes (Schwaha, 2020a). A previous morphological assessment demonstrated severe differences with victorellids (Braem, 1939) and it has become clear that sundanellids are not related to victorellids (Schwaha, 2020a). However, detailed morphological analyses are still pending. In this study, we analyse the morphology of two sundanellids to obtain more information on the morphological characters and hence the phylogenetic position of sundanellids.

2 | MATERIALS AND METHODS

S. sibogae (Harmer, 1915) was collected from the Lim Chu Kang mangrove habitat on Johor Strait, Singapore, on 8 May 2019. At this locality (1.4458° N, 103.7080° E), colonies form thick, dense bands around the bases of mangroves that are easily visible from a standing height. *Sundanella floridensis* sp. nov. was collected in the Fort Pierce Inlet of Indian River Lagoon, Fort Pierce, Florida, on 18 February 2019, attached to basal portions of Manatee grass blades (*Syringodium filiforme*). Specimens were either fixed in 4% paraformaldehyde in 0.1 mol L^{-1} phosphate buffer for approximately 1 h followed by several rinses in the buffer or in 2% glutaraldehyde in 0.1 mol L^{-1} phosphate buffer for several days.

Several colony pieces of both species were taken for histological sectioning and fluorescence staining and confocal laser scanning microscopy. Before processing for morphological studies, specimens were analysed and documented with either a Nikon SMZ25 stereomicroscope (Nikon) equipped with a Nikon DsRi2 microscope camera, or a Hirox RH-2000 (Hirox).

For histological sectioning, samples were dehydrated in acidified dimethoxypropane followed by several rinses in pure acetone. Afterwards, they were infiltrated into agar low-viscosity resin (LVR; Agar Scientific) via acetone as an intermediate. Embedded samples were serially sectioned with a HistoJumbo diamond knife (Diatome) on a Leica UC6 Ultracut (Leica Microsystems) at a section thickness of 1 μm (see also Ruthensteiner, 2008). Staining was conducted with toluidine blue. Stained sections were sealed with LVR and analysed and documented with a Nikon NiU compound microscope equipped with a Nikon DsRi2 microscope camera (Nikon).

For confocal laser scanning microscopy, specimens were incubated in a solution of 2% Triton-X and 2% dimethylsulphoxide in 0.1mol L^{-1} phosphate buffer for permeabilization overnight. For f-actin staining, phalloidin-coupled AlexaFluor 488 was applied at a concentration of 1:40 to the samples for 20–24 h followed by several rinses in the buffer. Rabbit anti-acetylated alpha tubulin antibodies were used in a concentration of 1:800 for staining neuronal elements and cilia. A secondary goat anti-rabbit AlexaFluor 568 antibody was used for labelling the first antibody at a concentration of 1:300. Samples were mounted with Fluormount G on standard microscope slides.

3 | RESULTS

3.1 | General morphology

Both sundanellid species generally show a creeping uniserial to cruciform growth pattern (Figures 1 and 2). Zooids in general

are large and in both species range over 1 mm in length. Strong zooidal differences are apparent in the higher peristome sizes in *S. sibogae* (1268–2707 µm, mean 1750 µm; Figure 1), whereas *S. floridensis* sp. nov. has lower peristomes (702–1067 µm, mean 1146 µm; Figures 2 and 3). Increased peristomial size in *S. sibogae* reduces the proximodistal zooidal axis attached to the substrate. This often results in zooids with only a short basal attachment site to the substrate whereas finger-like protrusions/peristomes contain the entire polypides (Figure 3a). In addition, the growth of the low-peristomial *S. floridensis* sp. nov. is denser and also shows frequent lateral buds in zooidal astogeny (Figure 2). In contrast, the investigated specimens of *S. sibogae* predominantly show uniserial growth in the proximodistal direction (Figure 1).

3.2 | Cuticle and interzooidal pores

The cuticle or ectocyst of sundanellids can be rather thin in certain areas but is considerably thick elsewhere. In the latter state, it usually appears multilayered, consisting of several parallel lamellae (Figures 4 and 5). Towards the frontal side of the aperture, the cuticle can show multiple wrinkles appearing as irregular branched structures (Figures 4b and 5b,c). These can also be evident as cuticular rings on the peristome of *S. floridensis* sp. nov. (Figure 2e,f). The cuticle transitional to and including the vestibular wall shows the highest degree of cuticular branching (Figure 4b).

Interzooidal communication areas are arranged in pore plates in *Sundanella*. In both species, two pore plates composed of

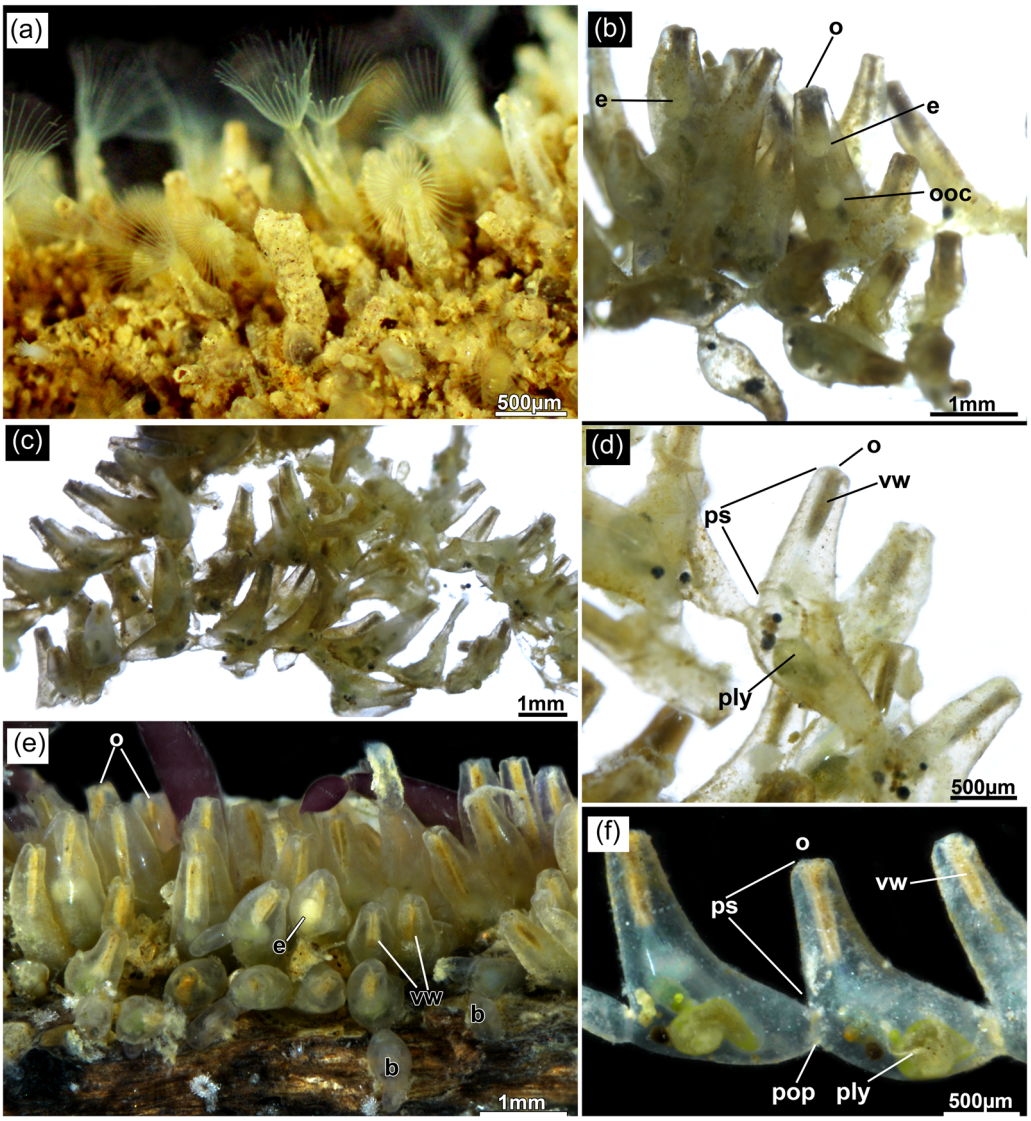

FIGURE 1 *Sundanella sibogae*, general overview. (a) Overview of a part of a live colony with protruded zooids attached to the original substrate. (b, c) Colony pieces detached from the substrate. (d) Close-up of a single zooid detached from the substrate showing the retracted polypide and vestibular wall. (e) Part of a colony with brooded embryo within the vestibular wall. (f) Close-up of a series of zooids. b, bud; e, embryo; o, orifice; ooc, oocyte; ply, polypide; pop, pore plate; ps, peristome; vw, vestibular wall.

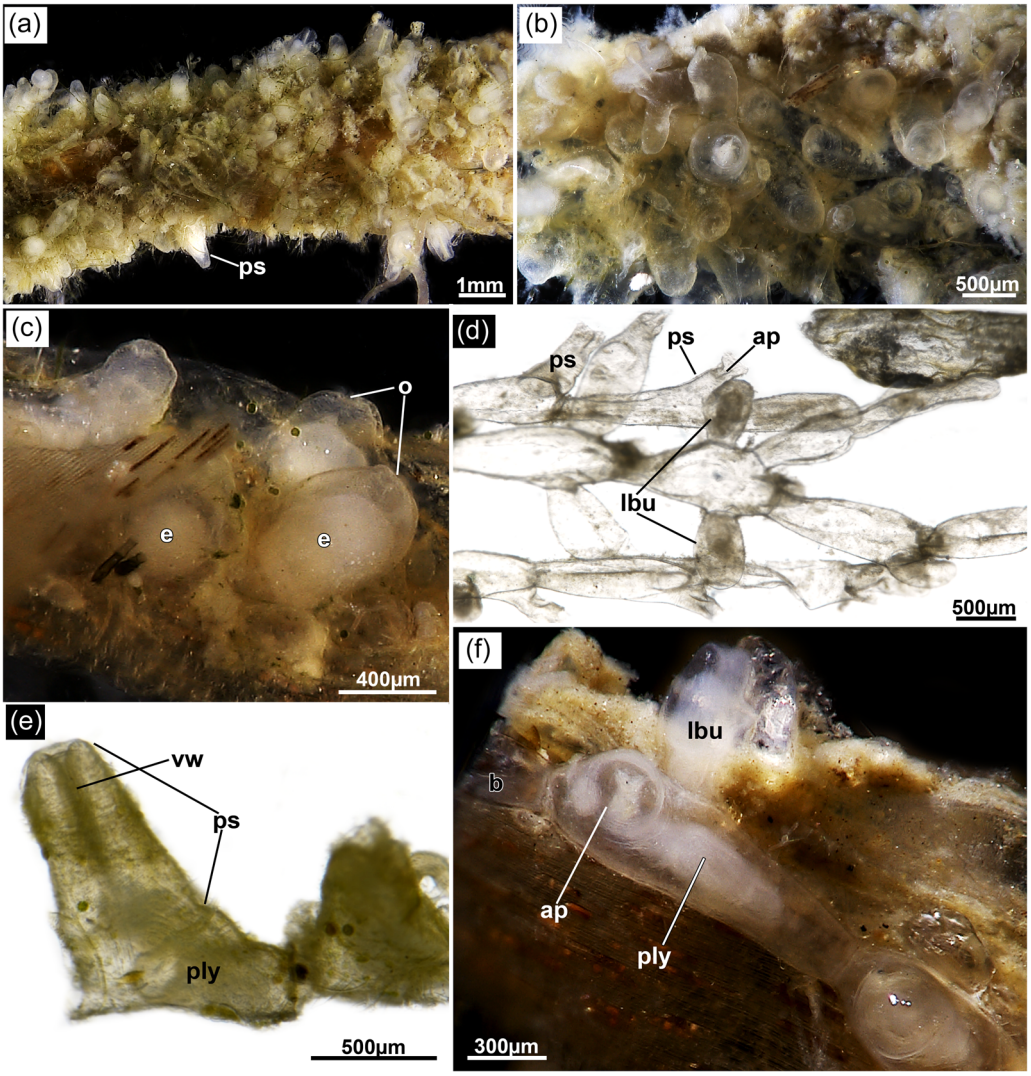

FIGURE 2 *Sundanella floridensis* sp. nov., general overview. (a) Overview of a colony attached to the substrate showing a dense arrangement of zooids with moderate to small peristomes. (b) Details of holotype colony showing the tight arrangement of zooids. (c) Lateral view showing brooded embryos within zooids. (d) Close-up of paratype 2 showing short peristomes in empty zooids and also lateral budding. (e) Lateral view of a single zooid showing cuticular wrinkles in the peristome. (f) Close-up of colony branch showing few zooids with short peristomes. ap, aperture; b, bud; e, embryo; lbu, lateral buds; o, orifice; ply, polypide; ps, peristome; vw, vestibular wall.

multiple interzooidal pores are located in the lateral walls (Figures 4a, 5d,f,g, and 6). Based on our current observations, the number of pores per plate varies from 10 to 13. Each pore is plugged with single special cells (Figures 4a and 5f) that are dumbbell-shaped, with the nucleus of the cell being in the proximal zooid. Besides the special cells, adjoining limiting cells can occur (Figure 4a). Their abundance seems to depend on the presence and state of peritoneal cells adjoining the endocyst lining. A series of funicular cords are often present and associated with pore plates (Figures 4a, 5d–f, 6a, 7a,b,d, and 8d). These can run as single or multiple, solid cords through the body cavity and usually attach to parts of the digestive tract (Figures 7a,b,d and 8a,b,d,e).

3.3 | Apertural area

The aperture is quadrangular in both sundanellid species (see Figures 2f and 3) and in retracted zooids inwards continues as a conspicuous vestibular wall with a wrinkled cuticle. In cross-section, the vestibular area is rectangular and widened in a lateral direction and more flattened in the proximodistal direction (Figure 9a,c). Proximally, the vestibular wall terminates with the diaphragm that is characterized by circular sphincter muscles (see also below, Figures 9b and 10b–d). The lining epithelium is highly vacuolated in *S. sibogae* (Figure 9) but highly glandular in *S. floridensis* (Figure 10a,c). These glands line the diaphragmal area of the tentacle sheath and form pouches or sac-like compartments. Many single glandular cells

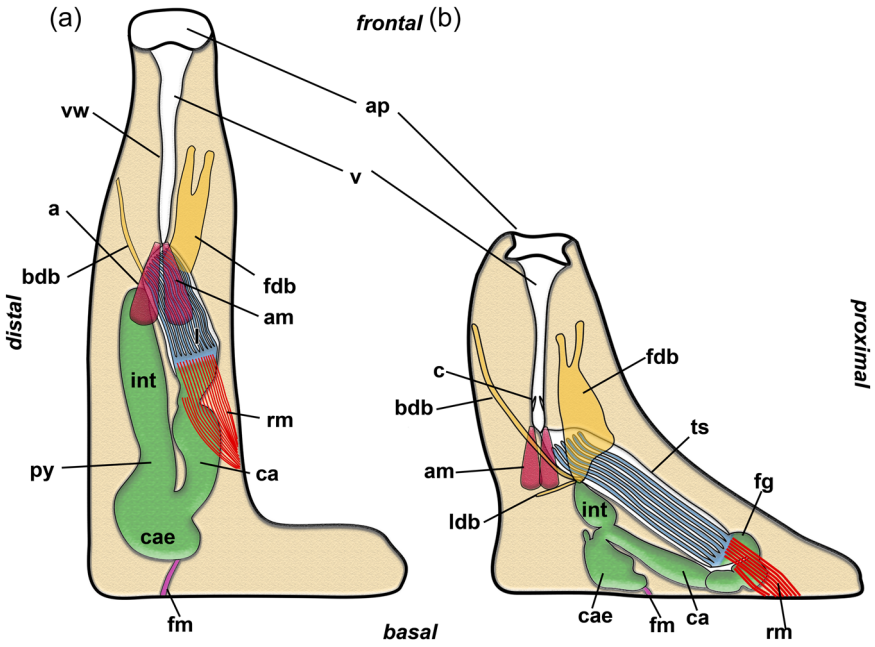

FIGURE 3 Schematic drawing of the two analysed species of *Sundanella sibogae* (a) and *S. floridensis* sp. nov. (b). a, anus; ap, aperture; bdb, basal duplicature band; c, collar; ca, cardia; cae, caecum; fg, foregut; fm, funicular muscle; int, intestine; l, lophophore, ldb, lateral duplicature band; py, pylorus; ts, tentacle sheath; v, vestibulum; vw, vestibular wall.

also appear clustered within the basal ECM of the glandular layer (Figure 10c). Slightly above the diaphragm an inconspicuous collar-fold projects distally into the vestibulum (Figure 10d).

Two lateral pairs of parietodiaphragmatic apertural muscles insert bilaterally at the diaphragm (Figures 3, 7, 8a,b,d, and 9a–d). Additional muscular duplicature bands arise from the tentacle sheath and project distally (in retracted zooids). A large, broad frontal duplicature band arises from the sheath in both species and splits into four single bands in its distal traverse (Figures 3, 7, 8, 9a,c, and 10a). On the basal side, two individual bands are present (Figures 3, 7, and 8). In *S. floridensis*, an additional pair of lateral duplicature bands projects frontodistally, rendering the number of duplicature bands in this species to six (Figures 3b and 8).

3.4 | Lophophore and digestive tract

Sundanellid lophophores are large and entail 30–31 tentacles in both species. In retracted zooids, the distal part of the lophophore, towards the diaphragm, is bent and convoluted (Figures 7b and 8c–e). The lophophoral base shows a distinct bilateral arrangement with two oral tentacles being elongated in the oral direction (Figure 11a).

The digestive tract commences from the lophophoral base with a mouth opening that enters the foregut, consisting of the pharynx and more proximally oesophagus (Figures 3, 7a,b, and 8d,e). Along the two elongated oral lophophoral base tentacles a median groove, the rejection strait, is present in the upper part of the pharynx. The junction between the foregut and midgut is characterized by the cardiac valve (Figure 12e). The cardia, as the first part of the midgut, can show highly variable proportions (see Figure 12c), which appears to be correlated with peristome size and is also reflected by a highly folded cardiac epithelium (Figure 12e). The main part of the stomach, the caecum, is short and has a short caecal pouch that bends proximally (Figures 3, 7a,b, 8c,e, 11b, and 13d). Distally, the midgut continues with the ciliated pylorus before entering the hindgut or intestine, which terminates with a vestibular anus close to the distal diaphragm (Figures 3, 7a,b, 8c–e, 10a, 11c, 12c, and 13b,c,e). In *S. floridensis*, the intestine is short (Figures 3b and 8c–e), whereas it is massive and extremely elongated in *S. sibogae* (Figures 3a and 7a,b). The anus in both species is vestibular and terminates close to the vestibular wall.

3.5 | Muscular systems

The muscular system can be divided into six different systems according to Schwaha and Wanninger (2018) and Schwaha (2020b):

(1) Body-wall-associated musculature in *Sundanella* comprises a series of thick and prominent parietal muscle bundles lateral to the polypide (Figures 12a,b and 14a,b). Muscular elements in the pore plates of the body walls were not encountered.
(2) Apertural musculature as bilateral, paired parietodiaphragmatic muscles that insert at the muscular diaphragm at the junction of the vestibular wall and tentacle sheath and the peritoneal duplicature bands extending distally from the tentacle sheath (see above, Figures 3, 7, 8, and 9a–c). Apart from the diaphragmatic sphincter, no vestibular wall muscles are present.
(3) Tentacle sheath muscles present as longitudinal muscle fibres that extend into the duplicature bands also distally (Figure 14b).

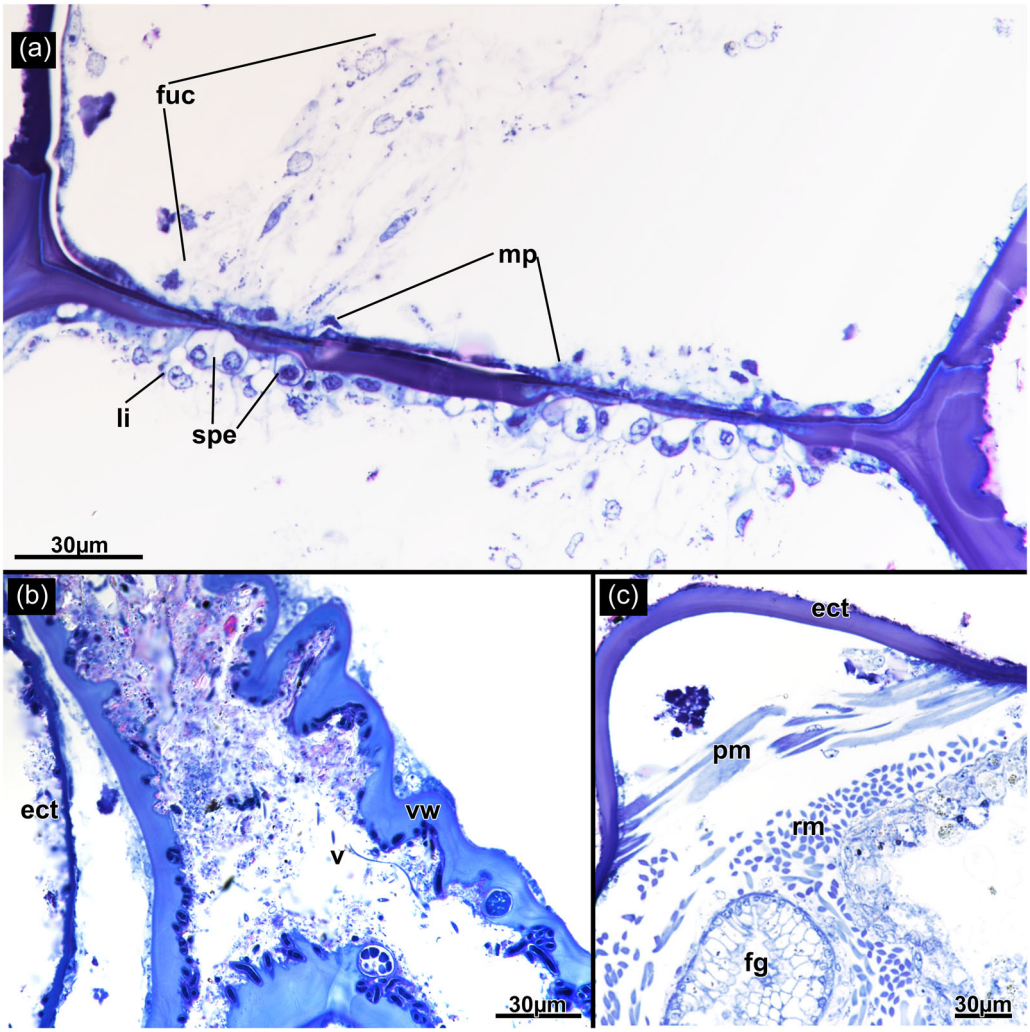

FIGURE 4 *Sundanella sibogae*. Details of the cuticle (ectocyst), pore plates and funicular strands; semithin sections, toluidine blue. (a) Section of two adjacent multiporous pore plates. (b) Vestibular area showing a thick cuticle, particularly in the vestibular wall showing a branched surface. (c) Thick multilayered cuticle and parietal muscle connected on both sides. ect, ectocyst; fg, foregut; fuc, funicular cords; li, limiting cell; mp, multiporous pore plate; pm, parietal muscles; rm, retractor muscles; spe, special cell; v, vestibulum; vw, vestibular wall.

(4) Digestive tract muscles consist of tightly arranged circular and striated foregut muscles (Figures 12c,d and 14c), a mix of longitudinal and circular muscles of the cardia and parts of the caecum (Figure 14d), followed by sole longitudinal muscles of the intestine (Figure 12a,b). At the proximal side of the caecum, a distinct funicular muscle connects the caecum to the basal body wall (Figures 3, 7a,b, 8c–e, and 13d).

(5) Lophophoral muscles consist of four lophophoral base muscles (abfrontal lophophoral base muscle, front-circular base mscle, V-shaped muscle and buccal dilatators, Figures 12d,f and 14c) and two tentacle muscles—the abfrontal and frontal tentacle longitudinal muscle. The frontal tentacle musculature is conspicuously thick, whereas the abfrontal ones start more distally within the lophophore (Figures 12a,d,f and 13).

(6) Retractor muscles present as multiple longitudinal bundles from the body wall to the lophophoral base and foregut (Figures 3, 12a,e, and 14b).

3.6 | Nervous system

Relatively few specimens were available for study, hence only a short depiction of the lophophoral base can be provided. The centre of the nervous system is located at the lophophoral base as a cerebral ganglion with a circum-oral nerve ring embracing the foregut (Figures 11a,b, 15, 16d–f, and 17). From the available data, two large pairs of neurite bundles emerge from the cerebral ganglion, the trifid nerves and the direct tentacle sheath nerves (Figures 15d,e and 17). A prominent mediovisceral neurite bundle from the ganglion (along with thinner lateral bundles) innervates the gut (Figure 15).

Tentacle innervation occurs via elongated, intertentacular radial neurite bundles that emerge from the ganglion or the circum-oral nerve ring. At least abfrontal and mediofrontal tentacle neurite bundles could be ascertained from the current data (Figure 15b,e,f).

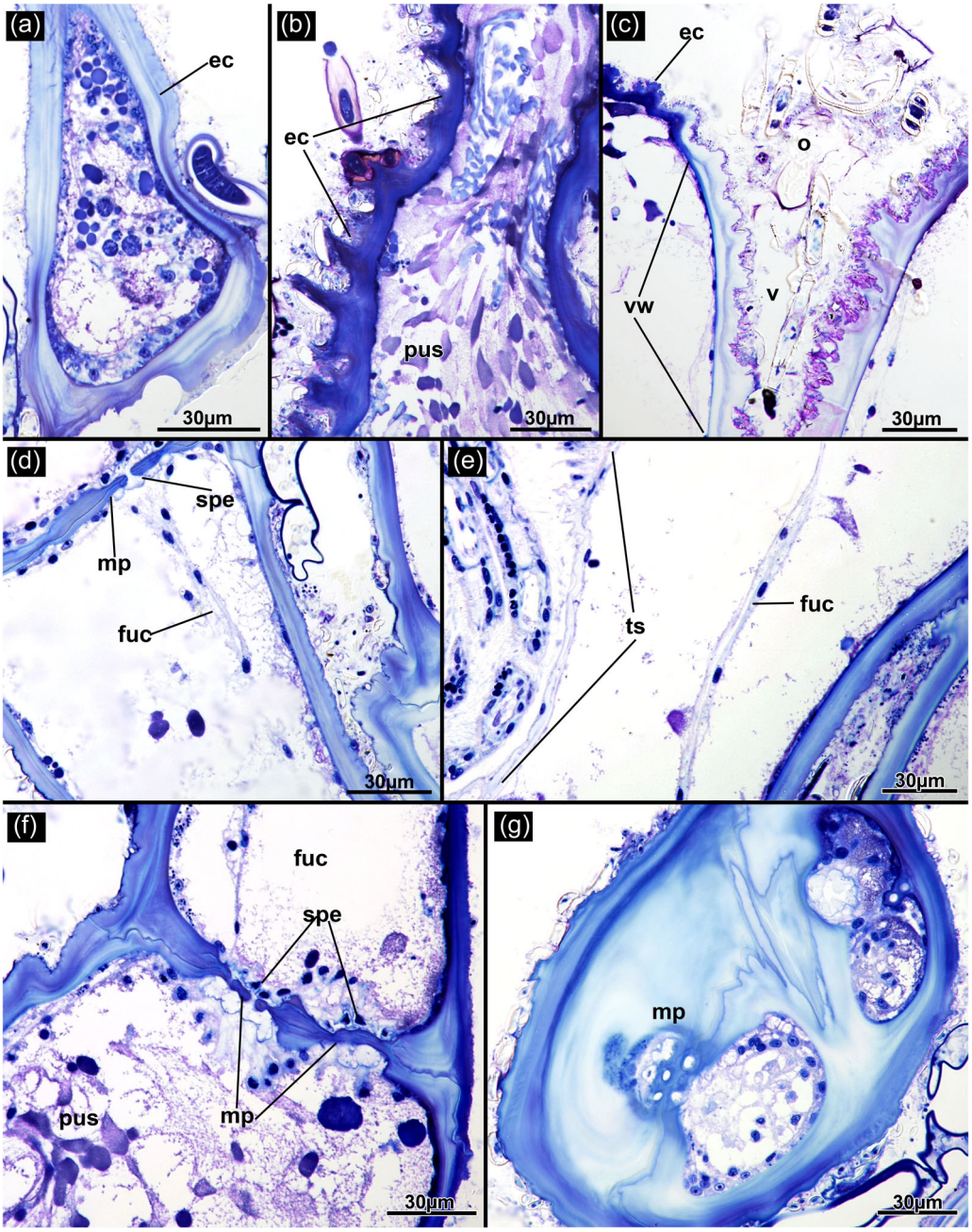

FIGURE 5 *Sundanella floridensis* sp. nov. Details of the cuticle (ectocyst), pore plates and funicular strands. (a) Thick cuticle showing multiple layers. (b) Cuticle with multiple ridged or folds increasing surface area. Note also the internal purplish slabs filling most of the body cavity. (c) Close-up of the orifice with the vestibular wall transitioning into the ectocyst. Note the rugged structure of the cuticular surface. (d) Multiporous pore plate with small special cells and a funicular cord attached to it. (e) Distinct funicular cord traversing the body cavity, next to the tentacle sheath. (f) Two adjacent multiporous pore plates. (g) Section showing multiple pores of one pore plate. ec, ectocyst; fuc, funicular cord; mp, multiporous pore plate; o, orifice; pus, purple slabs within the body cavity; spe, special cell; ts, tentacle sheath; v, vestibulum; vw, vestibular wall.

3.7 | Gonads, reproduction and embryos

Spermatogenic tissue appears to be widely spread and was found in various peristomial locations of the body wall (Figure 16a,b). Young spermatozoa and spermatids are easily distinguishable as grape-like arrangements, whereas riper sperm are characterized by their elongated tails (Figure 16b).

Various stages of oocytes and embryos were encountered in both species of *Sundanella*. In *S. floridensis*, only small developing oocytes and large brooded embryos were encountered (Figures 18 and 19), whereas larger oogenetic stages and less-developed embryos were found in *S. sibogae* (Figures 20 and 21).

Oocytes in *S. sibogae* are located on the body wall in the distal vestibular area of the zooid (Figure 20). Oocytes ripen in a

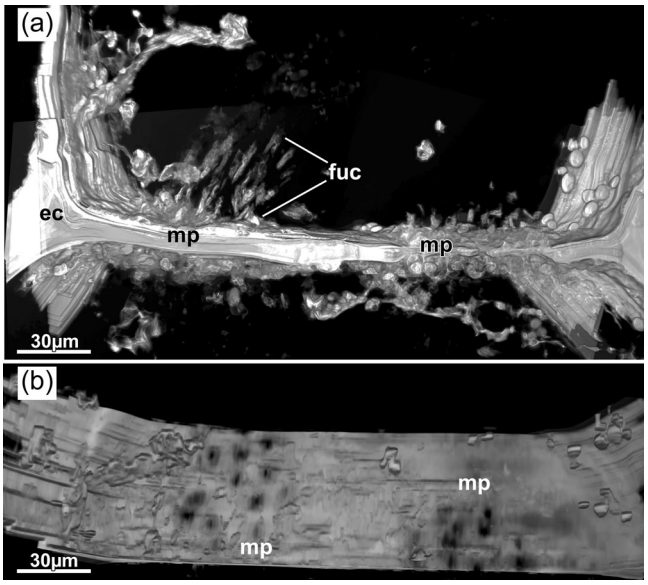

FIGURE 6 *Sundanella sibogae*. Histology-based 3D reconstruction of an interzooidal body wall and multiporous pore plate. (a) Lateral view of two multiporous pore plates with funicular cords attached. (b) View of the pores showing numerous single, small pores. 3D, three-dimensional; ec, ectocyst; fuc, funicular cords; mp, multiporous pore plate.

proximodistal direction and gradually enlarge. The surrounding follicle epithelium also gradually thickens and proliferates.

Macroscopically, larger embryos are distinguishable as large white bodies within the transparent zooids (Figures 1e and 2c). Early embryos in *S. sibogae* are embedded in the vestibular wall. Up to two or three embryos (~150 µm diameter) can be found located within a single zooid (Figure 21). The cuticle of each embryo displaces the cuticular lining of the vestibular wall, with the embryonic cuticle facing the vestibulum (Figure 21a,b). Each embryo in these vestibular pouches consists only of a few blastomeres.

In contrast, the embryos encountered in *S. floridensis* consist of multiple cells that are embedded in a body-wall invagination (Figure 19). This invagination is not associated with the vestibular wall, but with the free cystid wall in a zooid lacking any polypide remains. In its distal areas, two layers of the brood sac consisting of the outer peritoneum and inner epidermal part are discernible (Figure 19a,b). In the more enlarged and stretched areas around the embryo, a peritoneal layer is indistinguishable (Figure 19d–g). The embryo-sac wall, however, shows thick cells with a distinct acellular layer towards the brooded embryo (Figure 19d–g). Surrounding the embryo sac within the polypide-vacated zooid are multiple slabs of intensely stained, acellular materials (Figure 19).

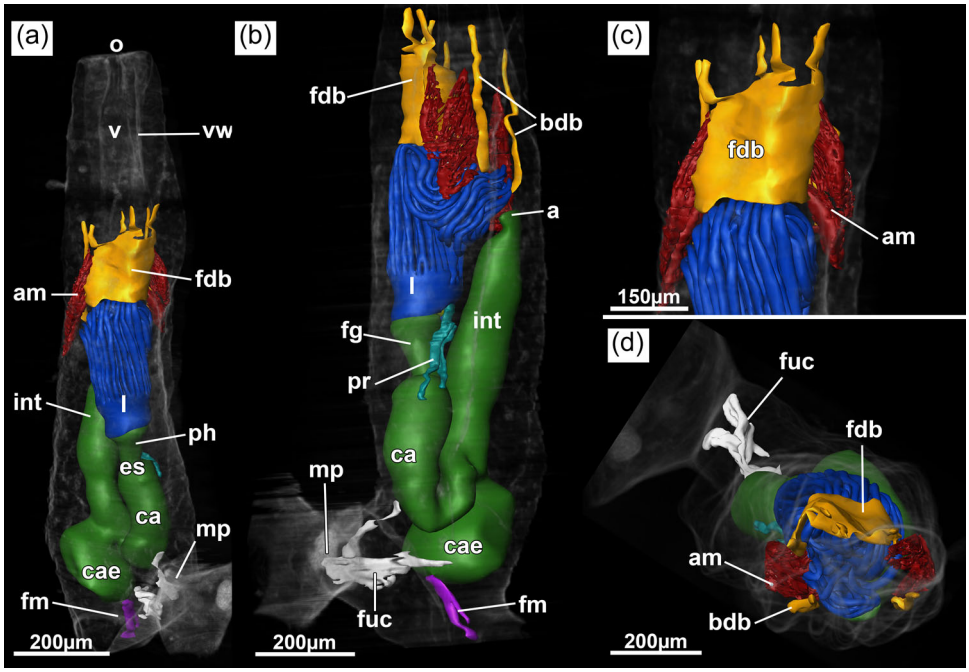

FIGURE 7 *Sundanella sibogae*. 3D-reconstruction based on a retracted zooid. (a) Lateral view of the zooid. (b) Lateral view of the zooid. (c) Close-up of the frontal duplicature band. (d) Frontal view of the aperture showing the bilateral arrangement of the musculature and also the bands. 3D, three-dimensional; a, anus; am, apertural muscles; bdb, basal duplicature band; ca, cardia; cae, caecum; es, oesophagus; fdb, frontal duplicature band; fm; funicular muscle; fuc, funicular cord; int, intestine; l, lophophore; mp, multiporous pore plate; o, orifice; ph, pharynx; pr, peritoneal ridges; v, vestibulum; vw, vestibular wall.

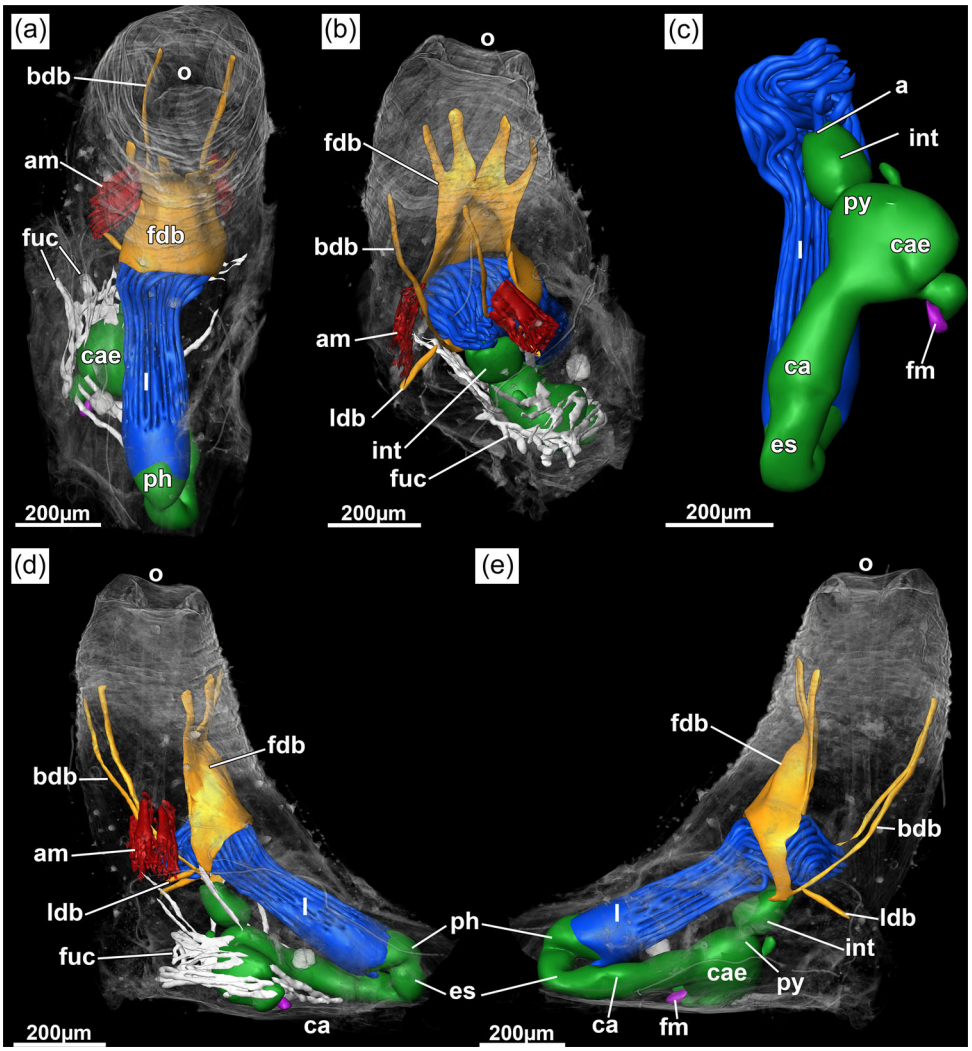

FIGURE 8 *Sundanella floridensis* sp. nov. 3D-reconstruction based on a retracted zooid. (a) Frontal view. (b) Oblique basodistal view. (c) Basal view of the digestive tract, lophophore and funicular muscle. (d) Left view of the zooid. (e) Right view of the zooid. 3D, three-dimensional; a, anus; am, apertural muscles; bdb, basal duplicature band; ca, cardia; cae, caecum; es, oesophagus; fm, funicular muscle; fuc, funicular cord; int, intestine; l, lophophore; ldb, lateral duplicature band; o, orifice; ph, pharynx; py, pylorus.

3.8 | Species description

Family Sundanellidae Jebram (1973).

Genus *Sundanella* Braem (1939).

Sundanella floridensis sp. nov.

lsid:urn:lsid:zoobank.org:pub:7859A66F-BB80-468D-B87E-03989EDDDCCD.

Victorella sibogae: Osburn (1940, p. 336).

Sundanella sibogae: Maturo (1957, p. 20), Figure 6; Shier (1964, p. 648), Figure 16; Winston (1982, p. 108), Figure 6; Santagata (2008, p. 356), Figure 5a,b.

3.8.1 | Type material

Holotype: colony sampled from the type locality on 'date', fixed in, stored in glutaraldehyde and stored in ethanol. Smithsonian Natural History Museum of Natural History number USNM 1593462. Paratypes USNM 1593463-1593466. Colonies were sampled together with the holotype Smithsonian number. Type locality: Fort Pierce Inlet of Indian River Lagoon, Fort Pierce, Florida.

3.8.2 | Etymology

The species name refers to the Floridian type locality of the species.

3.8.3 | Description

Colony repent with large zooids growing with primary growth in the proximodistal axis and frequent lateral buds. Zooids are approximately 1391 µm long and 352 µm wide; Peristome being short with a mean of 1146 µm length and lophophore with ~30–31 tentacles,

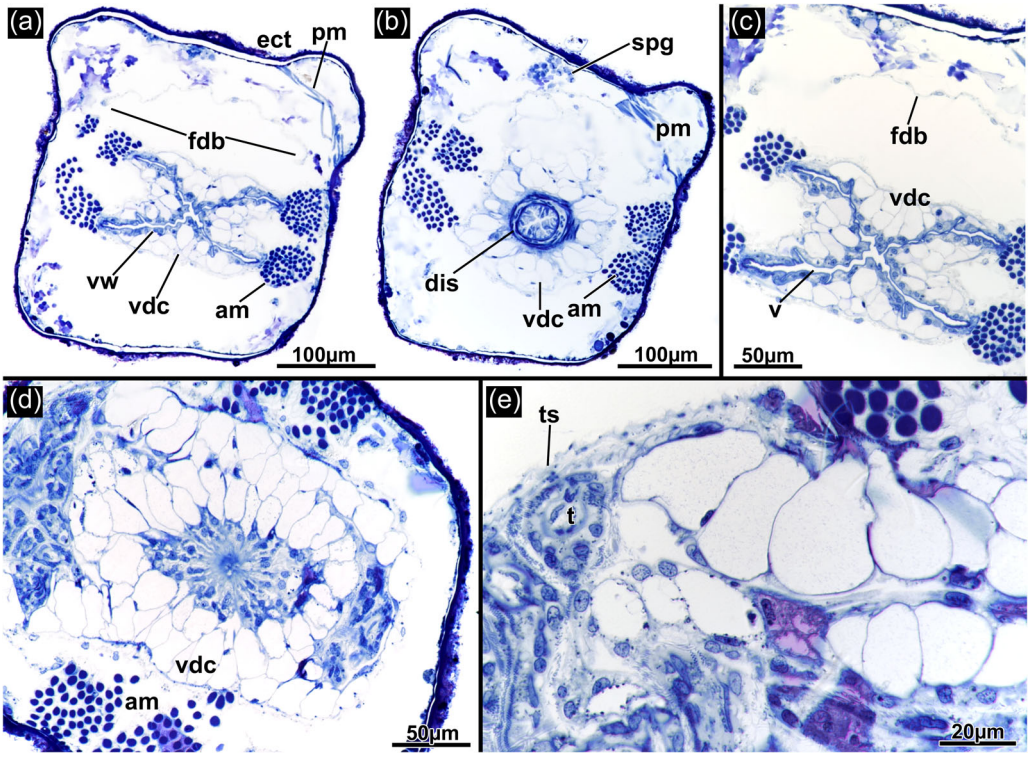

FIGURE 9 *Sundanella sibogae*. Details of the apertural area of retracted zooids. Semithin section, toluidine blue. (a) Cross-section of the lower apertural area showing a bilateral arrangement of the apertural muscles and the large frontal duplicature band. (b) Diaphragmatic sphincter surrounded by thick vacuolar cells. (c) Distal vestibular wall area showing vacuolated cells and the frontal duplicature band. (d) Detail of the vacuolated cells surrounding the diaphragmatic area. (f) Details of a single cell showing large vacuoles. am, apertural muscles; dis, diaphragmatic sphincter; ect, ectocyst; fdb, frontal duplicature band; pm, parietal muscles; spg, spermatogonia; t, tentacle; ts, tentacle sheath; v, vestibulum; vdc, vacuolar diaphragmatic cells; vw, vestibular wall.

bilateral with oral rejection tract. Digestive tract with elongated cardia, medium-sized caecum and anus vestibular. The funicular system is extensive, consisting of multiple complex branches in the proximal zooidal area. The apertural area is quadrangular with one pair of parietodiaphragmatic muscles on each side, six duplicature bands: one broad 'king-size' band splitting into four individual bands, two basal ones and two additional lateral bands emanating perpendicularly of the tentacle sheath from the others. Apertural glandular tissue is present in the diaphragmatic area of the tentacle sheath. Embryos white.

3.8.4 | Remarks

The high variability renders cystid characters highly questionable for species description and histology appears to be essential. *S. rosea* from Brazil was characterized based on its pink eggs and brooded embryos. The latter is clearly brooded in pouches of the vestibular wall. Tentacle number is similar to both other species of *Sundanella*, about 31. Most distinguishing is the very elongated size of *S. rosea* with up to 5 mm peristome lengths, frequent peristomial buds and its intertidal habitat (Vieira et al., 2014).

To prepare this manuscript we also studied preserved colonies of *Sundanella* from Florida and Brazil, as well as museum specimens from the Natural History Museum, London (NHMUK), including the paratype of *S. sibogae*. Although all museum specimens examined were brown in colour and mostly uniserial in colony form, close examination of zooid parameters indicated that Harmer's Indonesian material and other specimens comprised several different species under the name *S. sibogae*. The following NHMUK specimens were studied:

Victorella sibogae Paratype. 16.8.23.39 and 39a. Whole-mount slide in glycerine. SIBOGA Stat.64, 0–32 m. Kamboragi Bay, Tanah Djampeah, Monogr. 28A, p. 45, no. 451.B. Comments: zooids larger than those of Florida species, with side branching at an 80°–90° angle to the main growth direction.

Victorella sibogae (Harmer). 1965.1.47 Khor Al Bazani, Abu Dhabi, Trucial Coast, Persian Gulf. Mrs. G. Evans. Jar, preserved in alcohol. Comments: zooids are very large, crowded together and close to the Harmer specimen (above) in shape.

Victorella sibogae (Harmer). 1979.1.26.6 Murray Sound, Torres Straits, 15–20 fm. A. C. Haddon. Comments: zooids smaller and wider in proportion to length than those of Indonesian *S. sibogae*, with a squared-off orifice; one laterally branched zooid has budded at the same approximate angle as the Harmer specimen.

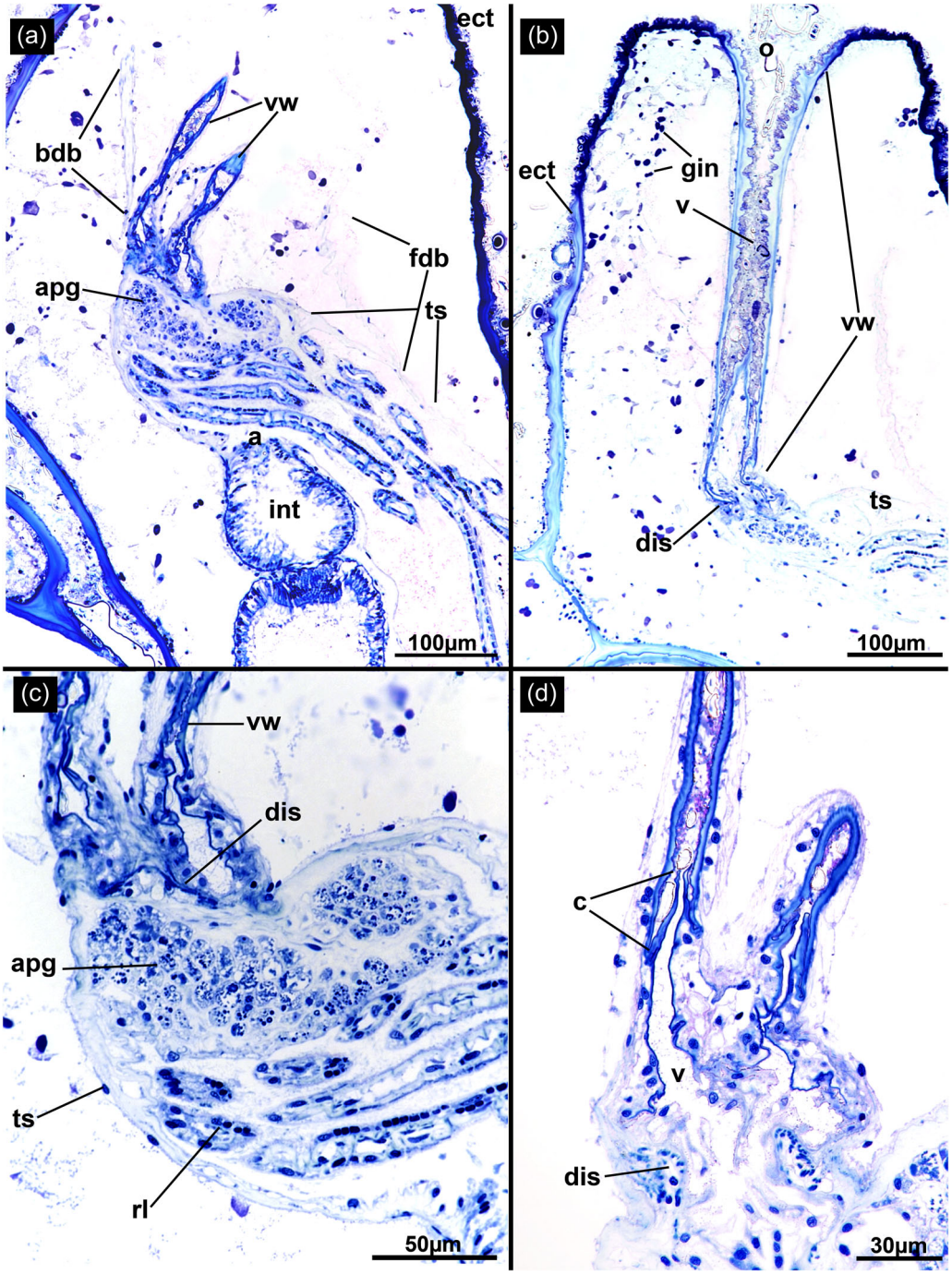

FIGURE 10 *Sundanella floridensis* sp. nov. Details of the apertural area of retracted zooids. (a) Distal tip of tentacle sheath showing the transition into the vestibular wall, duplicature bands and the vestibular anus. (b) Orifice entering the vestibular wall. Note also the rugged cuticle. (c) Details of apertural glands associated with the tentacle sheath below the diaphragm. (d) Transition of the tentacle sheath into the vestibular wall showing the diaphragmatic sphincter and vestigial vestibular collar. a, anus; apg, apertural glands; bdb, basal duplicature band; c, collar, dis, diaphragmatic sphincter; ect, ectocyst; fdb, frontal duplicature band; gin, granular inclusions; int, intestine; o, orifice; rl, retracted lophophore; ts, tentacle sheath; v, vestibulum; vw, vestibular wall.

Victorella sp. 32.12.19.39 (part) SV06. Colman-Tandy Coll. Dry Tortugas, no. 173. Stained, cleared whole-mount slide. Comments: This is *Sundanella floridensis;* no side branching.

3.8.5 | Distribution

West-Atlantic coast, North Carolina, Florida, Puerto Rico, Gulf of Mexico.

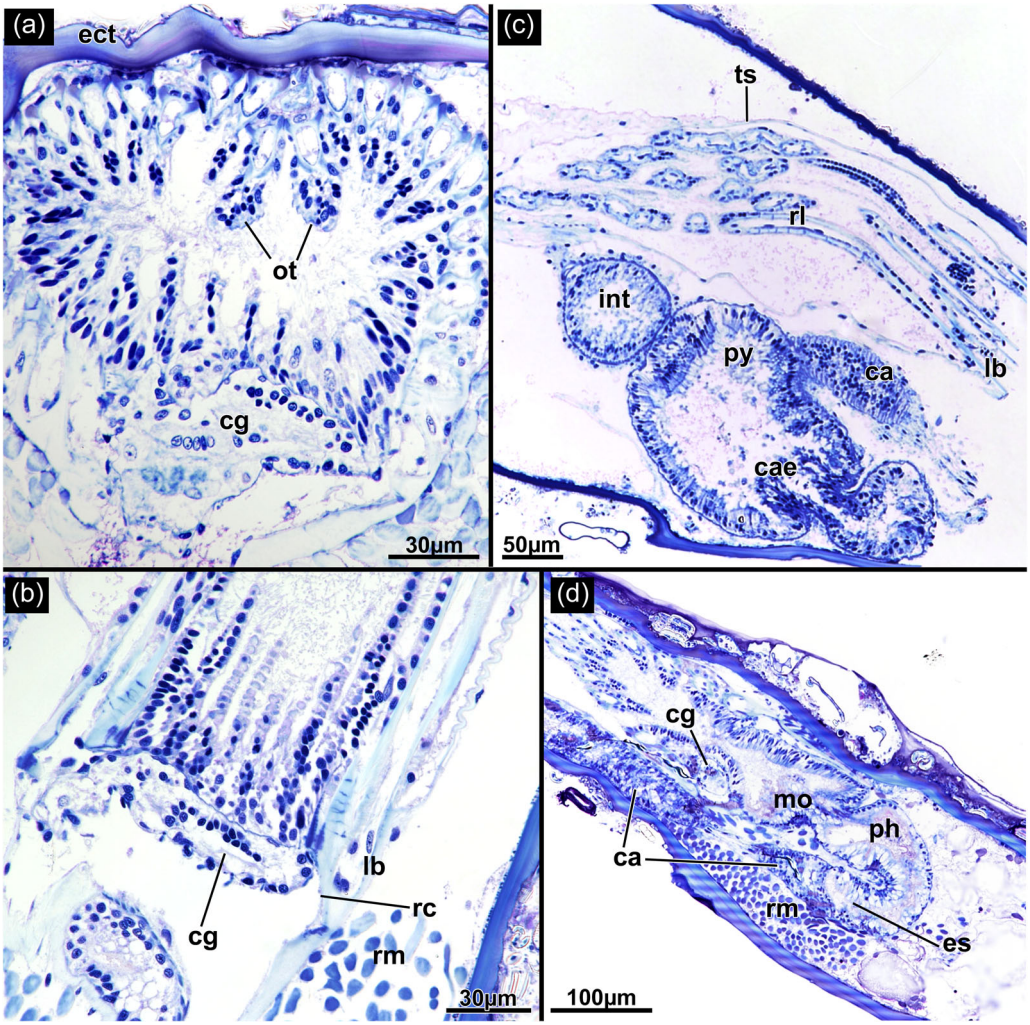

FIGURE 11 *Sundanella floridensis* sp. nov. Histological details of the lophophore and gut. (a) Cross-section of the lophophoral base showing the bilateral lophophore with the enlarged oral tentacles. (b) Longitudinal section showing the cerebral ganglion at the lophophoral base. (c) Longitudinal section showing most parts of the mid- and hindgut. (d) Longitudinal section showing the foregut. a, anus; ca, cardia; cae, caecum; cg, cerebral ganglion; ect, ectocyst; es, oesophagus; int, intestine; lb, lophophoral base; mo, mouth opening; ot, oral tentacles; ph, pharynx; py, pylorus; rc, ring canal; rl, retracted lophophore; rm, retractor muscles; ts, tentacle sheath.

4 | DISCUSSION

4.1 | General morphology

The general colony structure indicates a slight difference between the two analysed species, with *S. sibogae* having longer peristomes and fewer lateral buds, in contrast to the short-stubbed *S. floridensis* with more frequent lateral buds. However, as indicated by previous investigations, such characters appear rather random and can occur in both of these species (Harmer, 1915). Hence, general colony morphology provides less-suitable specific characters. In general, colony morphology, particularly peristome size, can show significant differences within species of the same genera, but also within the same species (Braem, 1951; Jebram, 1982).

Previous reports of West Atlantic species found colonies with zooids consisting mostly of elongated peristomes (Puerto Rico: Osburn, 1940; North Carolina: Maturo, 1957), whereas material from Florida showed short to moderately long peristomes (Shier, 1964; Winston, 1982). In intertidal and subtidal collections made on the central east coast of Florida, most colonies of *Sundanella* are small, encrusting seagrass, algae, hydroid stems and holdfasts. They have also been reported from fouling panels on the Gulf coast of Tampa, Florida (Bros, 1987). The large (up to 1.5 mm), stout translucent white-to-tan-coloured zooids bud in attached uniserial rows along the substratum. Each new zooid is produced from the distal end of its predecessor, with only an occasional lateral branch. Specimens from North Carolina were also reported to form peristomial buds (Maturo, 1957), a feature otherwise found only in *S. rosea* (Marcus, 1937; Vieira et al., 2014). Peristomial budding was often considered to be a character of victorellids (Jebram, 1973), but has also been shown in the genus *Bockiella* (Hayward, 1985). The large variation in zooidal morphology could be substrate-related as

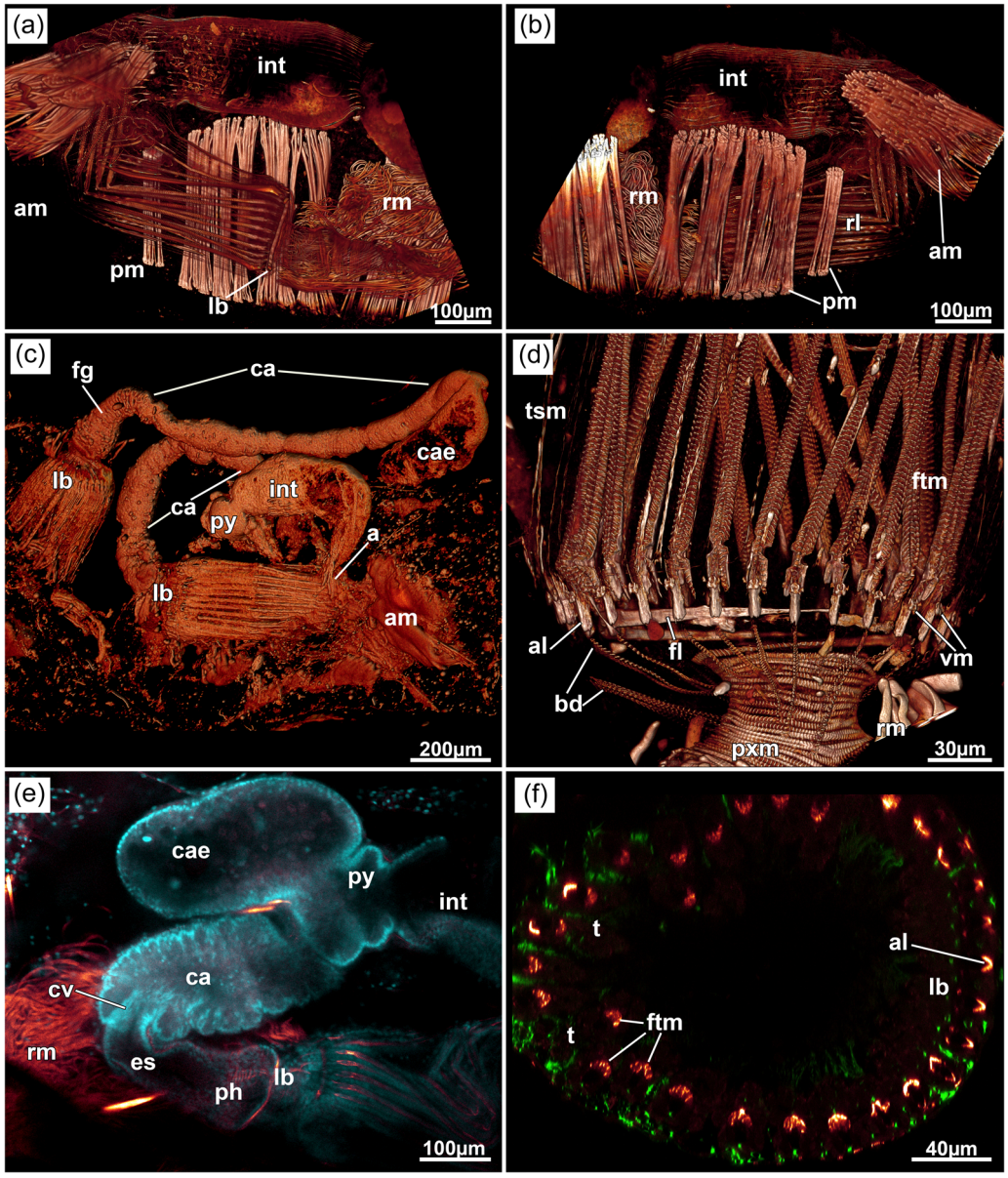

FIGURE 12 *Sundanella sibogae*. Myoanatomical aspects, phalloidin staining of musculature and nuclear counterstaining (DAPI) and confocal laser scanning microscopy of retracted zooids. (a) Lateral view showing massive parietal muscles and extensive intestine. (b) Same as in (a) but from the opposite side. (c) View of dissected zooids showing the extreme extensibility of the cardiac region. (d) Lateral view of the lophophoral base. (e) View of the proximal gut showing the folded epithelium of the cardiac area. (f) Cross-section of the lophophoral base showing lophophoral base and tentacle muscles. a, anus; al, abfrontal lophophoral base muscle; am, apertural muscles; bd, buccal dilatator; ca, cardia; cae, caecum; cv, cardiac valve; db, duplicature band; es, oesophagus; fg, foregut; fl, frontal lophophoral base muscle; fm, funicular muscle; ftm, frontal tentacle muscle; int, intestine; lb, lophophoral base; ph, pharynx; pm, parietal muscles; pxm, pharyngeal musculature; py, pylorus; rl, retracted lophophore; rm, retractor muscle; t, tentacle; tsm, tentacle sheath muscles; vm, V-shaped lophophoral base muscles.

individual zooids with enlarged peristomes require less space on the substrate. Substrate limitation and large peristomes on the other hand might be the cause for peristomial budding.

Large peristome size in particular had been previously used as a character for assigning the genus *Sundanella* to victorellids, as also indicated in its initial assignment to the genus *Victorella* (Harmer, 1915). As first demonstrated by the detailed morphological analysis of Braem (1939), who also erected the genus *Sundanella*, it was evident that there are multiple characters emphasising that *S. sibogae* shows major differences to victorellids (see also below).

4.2 | Cuticle and apertural area

The cuticle is thick in *Sundanella*, much thicker than in victorellids as previously noted (Braem, 1939). Thick, often multilayered cuticles are common in alcyonidioidean ctenostomes (see Decker et al., 2021;

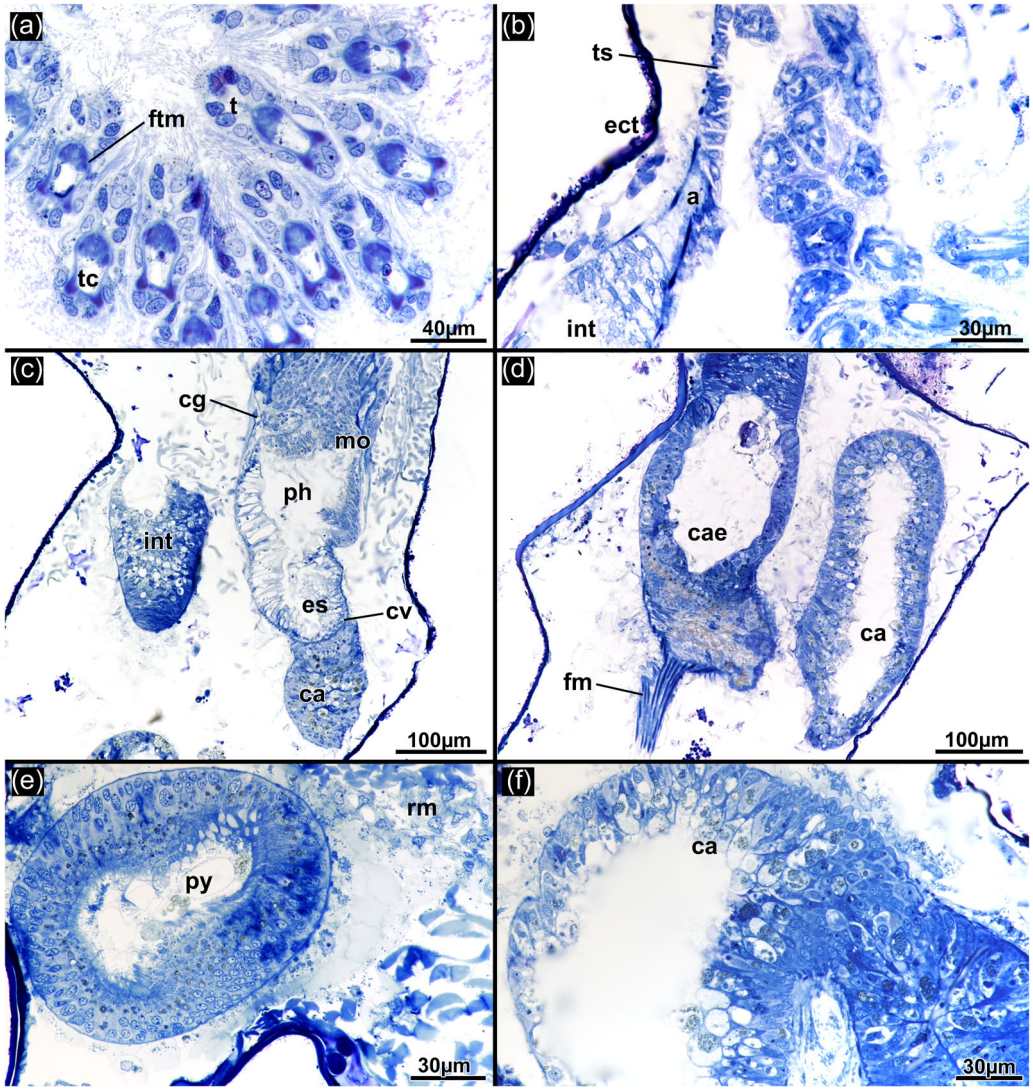

FIGURE 13 *Sundanella sibogae*. Histological details of the lophophore and gut. (a) Cross-section of several tentacles. (b) Oblique section showing the anus entering the tentacle sheath. (c) Longitudinal section showing the foregut and anally situated cerebral ganglion at the lophophoral base. (d) Longitudinal section showing the midgut including the prominent funicular muscle. (e) Cross-section of the pyloric area showing its internal ciliation. (f) Details of the cells of the caecum. a, anus; ca, cardia; cae, caecum; cg, cerebral ganglion; cv, cardiac valve; ect, ectocyst; es, oesophagus; fm, funicular muscle; ftm, frontal tentacle muscle; int, intestine; mo, mouth opening; ph, pharynx; py, pylorus; rm, retractor muscle; t, tentacle; tc, tentacle coelom; ts, tentacle sheath.

Matricon, 1960; Schwaha, 2021; Schwaha, Grischenko, et al., 2020). Particular cuticular branching as found in the cuticle of *Sundanella* has been found in *Haywardozoon* (Schwaha, Grischenko, et al., 2020) and species of the genus *Pherusella* (Decker et al., 2021).

Multiporous interzooidal pore plates are generally typical of cheilostome bryozoans (Cheetham & Cook, 1983; Martha et al., 2020), but were also found in the ctenostomes *Sundanella* and *Pherusella* (see Schwaha, Ostrovsky, et al., 2020). Recently, they were also confirmed for the flustrellidrid genera *Flustrellidra*, *Elzerina* and *Bockiella* (Schwaha, 2021). The number of pores varies in the different genera and in pherusellids can be even species-specific (Decker et al., 2021). In the latter, several species also show a distinct cuticular rim around each pore, which has not been observed in such form in other ctenostomes. The current study showed an average of 10–13 pores in each pore complex. Along with many other characters, these pore complexes are again a unifying character of all these multiporate ctenostomes.

The frontal 'king-size' duplicature band splitting into four individual bands has so far only been found in the flustrellidrid genus *Elzerina* and less conspicuously in *Flustrellidra* (Schwaha, 2021). A similar broad frontal duplicature band is also present in the closely related multiporate pherusellids (Decker et al., 2021). The number of duplicature bands varies among ctenostome bryozoans, with four being the basic set usually present (Schwaha, 2020a), which is also the case of *S. sibogae*. Six duplicature bands, as in *S. floridensis* sp. nov., are rare and have only been found in *Arachnidium fibrosum* in ctenostomes (Schwaha & De Blauwe, 2020). In contrast to *A. fibrosum*, the additional lateral pair of bands of *S. floridensis* has a

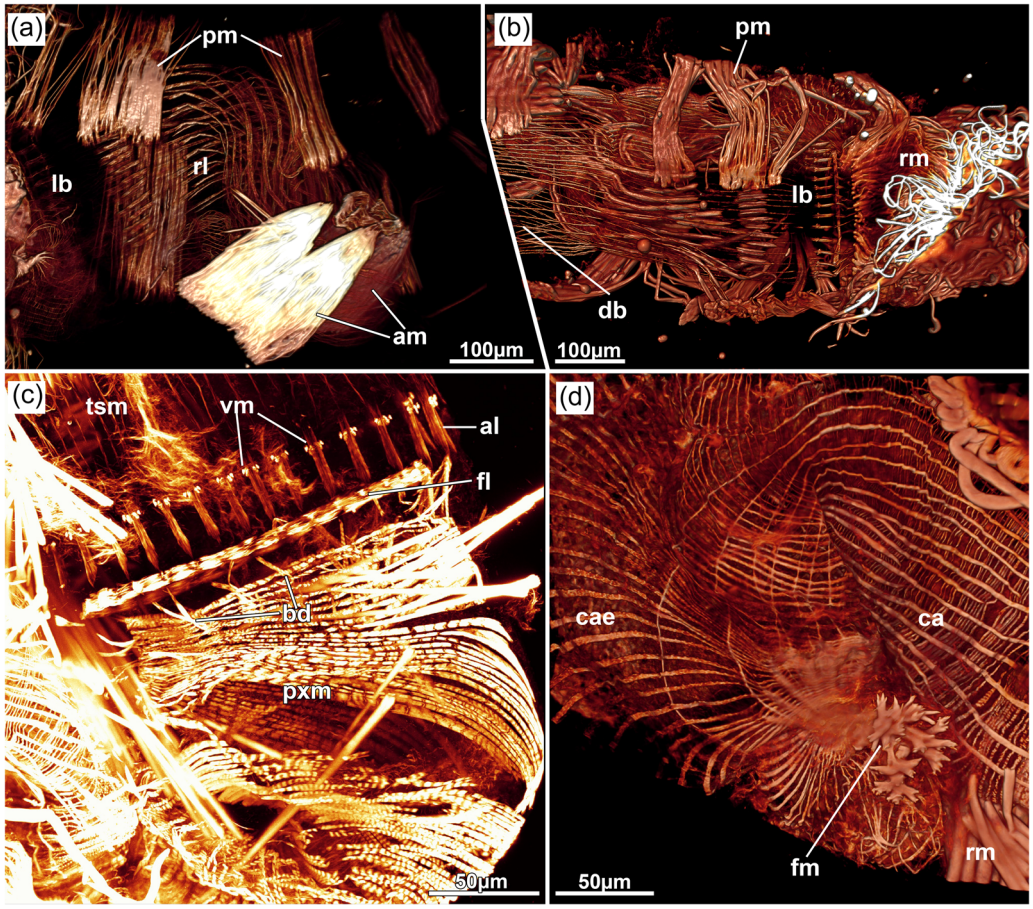

FIGURE 14 *Sundanella floridensis* sp. nov. Myoanatomical aspects, phalloidin staining and confocal laser scanning microscopy of retracted zooids. (a) Lateral view of a zooid showing prominent parietal and apertural muscles. Note also the diaphragmatic sphincter where the apertural muscles (parietodiaphragmatic muscle) insert. (b) Retracted zooid with distal thick duplicature bands emanating from the tentacle sheath. (c) View of the lophophoral base. (d) Detail of the midgut showing a thick funicular muscle from the caecum. al, abfrontal lophophoral base muscle; am, apertural muscles; bd, buccal dilatator; ca, cardia; cae, caecum; db, duplicature band; fl, frontal lophophoral base muscle, fm, funicular muscle; lb, lophophoral base; pm, parietal muscles; pxm, pharyngeal musculature; rl, retracted lophophore; rm, retractor muscle; tsm, tentacle sheath muscles; vm, V-shaped lophophoral base muscles.

different trajectory and runs more or less perpendicular to the direction of the remaining bands. Victorellid ctenostomes, to which the genus *Sundanella* has been previously often assigned (see d'Hondt 1983), lack duplicature bands entirely (Schwaha et al., 2011).

Apertural muscles were considered to have radial symmetry in *Sundanella* (Jebram, 1973), contrary to the reports of Braem (1939) and Marcus (1941) who found a bilateral arrangement in *Sundanella*. In accordance with the latter, only parietodiaphragmatic muscles are present and there are no distally inserting apertural muscles such as the parietovestibular ones seen in other ctenostomes (Schwaha & Wanninger, 2018; Schwaha et al., 2011). A single pair of apertural muscles, in the form of enlarged parietodiaphragmatic muscles, has also been shown in *S. rosea* (Marcus, 1941) and is otherwise only found in pherusellids (Decker et al., 2021), the genera *Elzerina*, *Flustrellidra*, *Bockiella* (Schwaha, 2021) and *Alcyonidium* (Prouho, 1892; Silbermann, 1906).

The diaphragmatic area is always characterized by a sphincter muscle in all bryozoans including ctenostomes (see Schwaha, 2020b). The two sundanellid species differ with highly vacuolated cells being present only at the diaphragm of *S. sibogae*, as already indicated by Braem (1939). Such vacuolated cells are unusual but have been reported for *Bockiella* sp. (Schwaha, 2021) and *Arachnidium fibrosum* (Schwaha & De Blauwe, 2020). The function of these cells remains unknown, but as the large vacuole does not seem to have any apparent content as in glandular cells, they might have a turgescent function.

The collar is a common feature of all gymnolaemates and can often show various degrees of reduction, especially among cheilostomes (Schwaha, Ostrovsky, et al., 2020). Among ctenostomes, it exhibits different shapes, such as a simple pleated fold or a strongly folded long structure obstructing the vestibulum (McKinney & Dewel, 2002). In most clades, it projects directly from the diaphragmatic region distally, but in mutliporate ctenostomes it originates slightly above the diaphragm, directly from the vestibular wall, a condition recently termed 'vestibular collar' versus 'diaphragmatic collar' (Schwaha, 2021). Our results on *Sundanella* also proved the presence

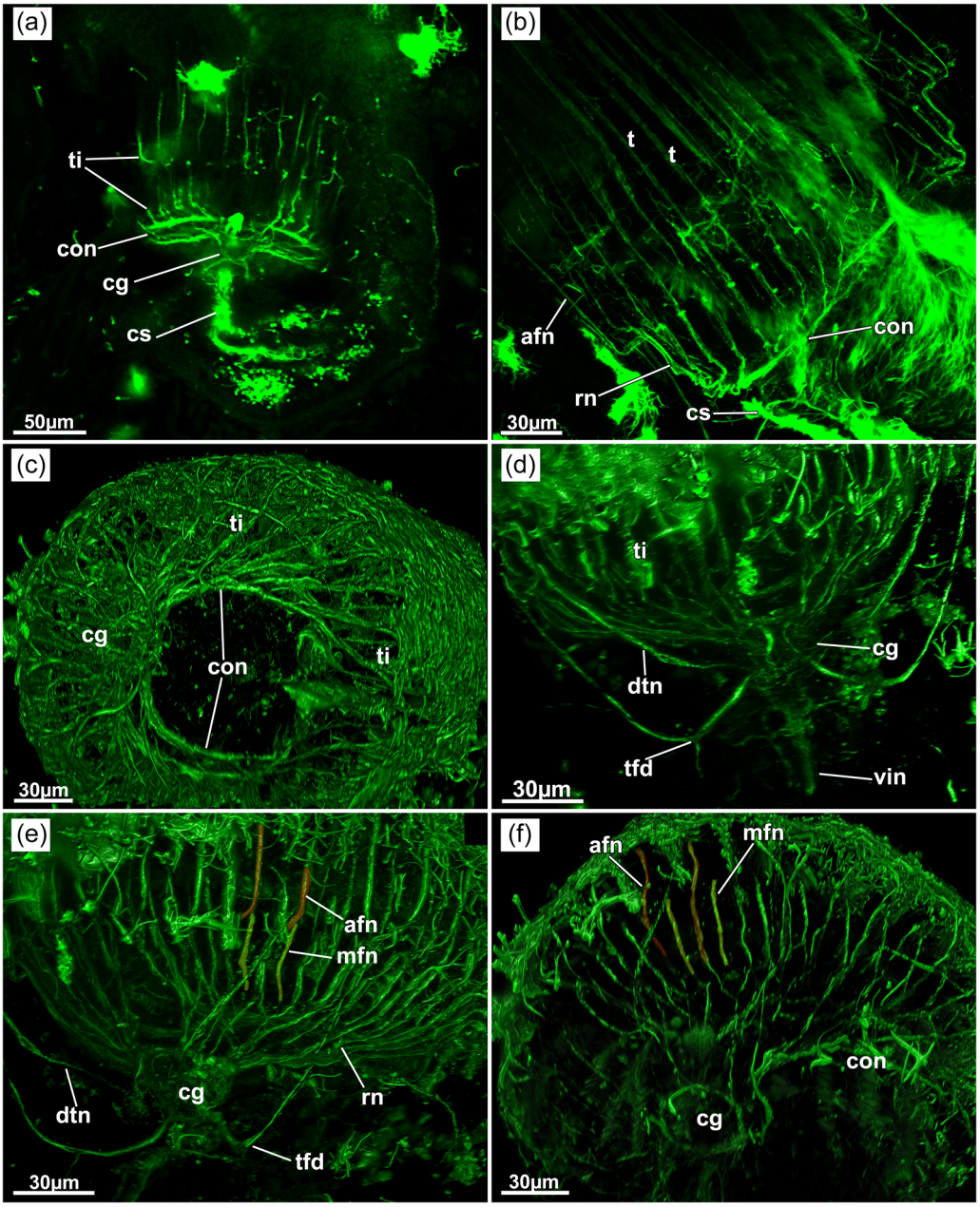

FIGURE 15 Acetylated alpha tubulin stainings of *Sundanella floridensis* sp. nov. (a, b) and *S. sibogae* (c–f). Volume renderings based on confocal laser scanning microscopy stacks. (a) Anal view of the lophophoral base. (b) Lateral view of the lophophoral base. (c) Basal view of the cerebral ganglion and circum-oral nerve ring. (d) Detailed anal view of the lophophoral base. (e) Details of the tentacle innervation from the anal side. (f) Details of tentacle innervation from the basal side. afn, abfrontal neurite bundle; cg, cerebral ganglion; con, circum-oral nerve ring; cs, ciliary street; dtn, direct tentacle sheath nerve; rn, radial nerve; t, tentacle; tfd, trifid nerve; ti, tentacle innervation; vin, visceral innervation.

of a vestibular collar, adding another synapomorphic feature of multiporate ctenostomes. In contrast, victorellids have a long, setigerous and diaphragmatic collar (Braem, 1951).

The discovery of glands in the apertural area of *S. floridensis* is exceptional and is the first finding in any ctenostome bryozoan. Glandular tissues designated as vestibular glands have been found in several cheilostome species (Calvet, 1900; Harmer, 1902; Lutaud, 1964; Marcus, 1939; Waters, 1894), although few were located in the tentacle sheath similar to *S. floridensis*. The close proximity of these glandular pouches in the vicinity of the diaphragm indicates that gymnolaemate gland tissue is not merely restricted to the vestibular area, but extends somewhat more proximally. Distal tentacle-sheath-associated glandular tissue has been previously reported in other cheilostomes (Lutaud, 1964). As there is a larger variation in the presence of these specific glandular tissues, we propose herein the term 'apertural glands' in contrast to vestibular glands that would solely exit into the vestibular area, to include the non-vestibular glands such as those in the tentacle sheath. It is

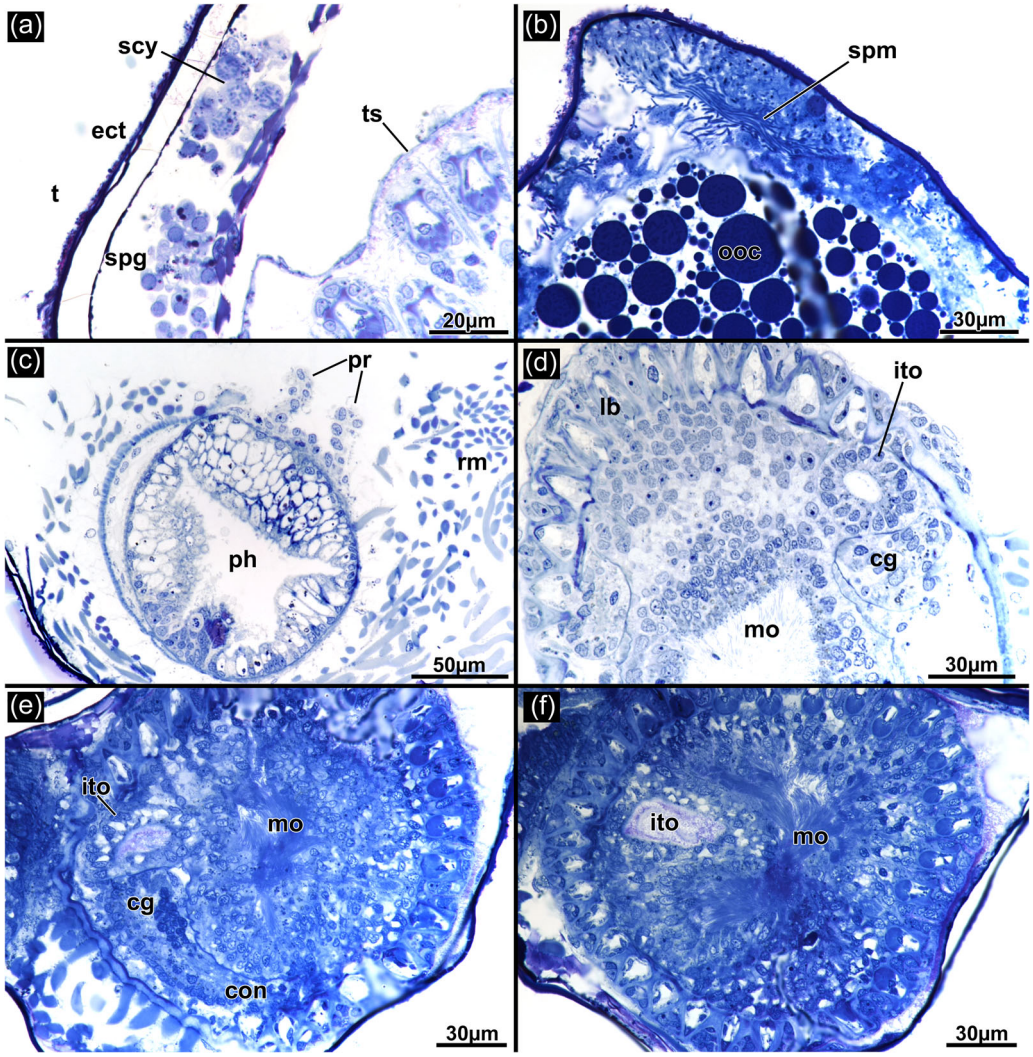

FIGURE 16 *Sundanella sibogae*, spermatogenesis and intertentacular organ. (a) Early spermatocytes in the distal body wall area. (b) Advanced spermiogenesis and a large oocyte. (c) Cross-section of the pharynx showing the ciliated peritoneal ridges on the anal side. (d) Lophophoral base showing the intertentacular organ close to the cerebral ganglion. (e, f) Different sections of the intertentacular organ epithelium more proximally (e) and distally (f) showing conspicuous inclusion and internal lining. cg, cerebral ganglion; con, circum-oral nerve ring; ect, ectocyst; ito, intertentacular organ; lb, lophophoral base; mo, mouth opening; ooc, oocyte; ph, pharynx; pr, peritoneal ridges; rm, retractor muscles; scy, spermatocytes; spg, spermatogonia; spm, sperm; ts, tentacle sheath.

interesting to note that vestibular glands were typically considered apomorphic for cheilostomes (e.g., Banta, 1975; Schwaha, Ostrovsky, et al., 2020). The presence of such glands in ctenostomes indicates either that they evolved independently or are shared with the still-unknown candidate for recent ctenostomes most closely related to cheilostomes.

4.3 | Lophophore and digestive tract

The lophophore of *Sundanella* is conspicuous in showing a high number of tentacles (>30) and a bilateral arrangement with enlarged oral tentacles forming the rejection tract, which has previously been observed by Braem (1939). The general structure of the lophophore is identical to flustrellidrid (Atkins, 1932; Schwaha, 2021) and pherusellid ctenostomes (Decker et al., 2020, 2021). In contrast, all victorellids generally possess eight tentacles and do not show any bilateral arrangement.

The digestive tract in both sundanellids is similar with respect to the foregut and shows a typical vestibular anus. The cardiac region and the intestine show differences within the genus, with the cardia being elongated in *S. floridensis* and short, but folded, in *S. sibogae* and the intestine unusually huge in *S. sibogae*. Such a large intestine has not been reported for any other ctenostome species. In *S. rosea*, the cardia is also elongated and the intestine is a small area terminating with a vestibular anus (Marcus, 1941). The caecum is of moderate size in all three species. The general arrangement, particularly with the vestibular anus, is reminiscent of alcyonidiid, flustrellidrid and pherusellid ctenostomes (Schwaha, 2020c). In contrast to the latter, the caecum is slightly larger, but not as large and elongated as in

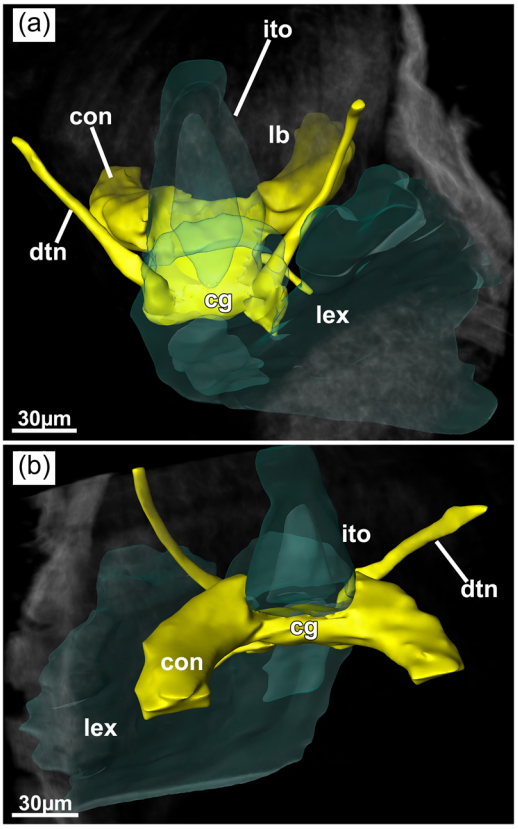

FIGURE 17 *Sundanella sibogae*. Histology-based 3D reconstruction of the intertentacular organ. (a) Anal view. (b) Oral view). 3D, three-dimensional; cg, cerebral ganglion; con, circum-oral nerve ring; dtn, direct tentacle sheath nerve; ito, intertentacular organ; lb, lophophoral base; lex, lateral peritoneal extension.

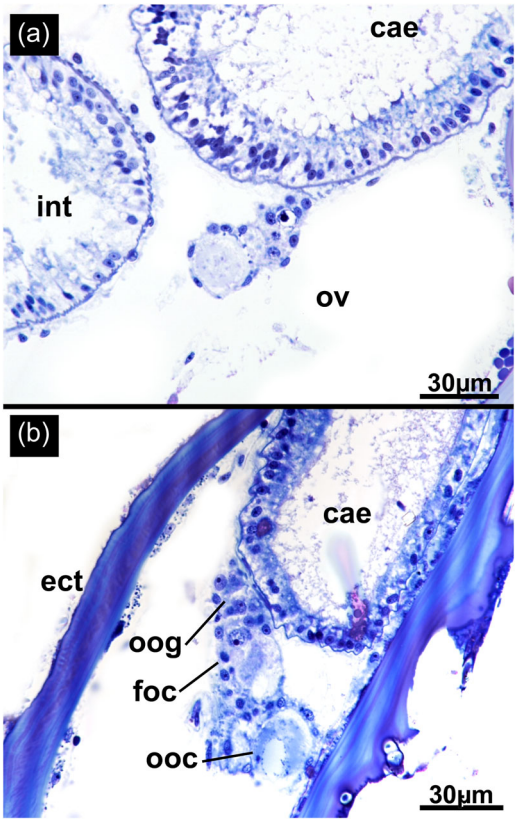

FIGURE 18 *Sundanella floridensis* sp. nov. Early oogenetic stages. (a) Peritoneal strand with very early oogenetic stages. (b) Series of multiple different oogenetic stages. cae, caecum; ect, ectocyst; foc, follicle cells; int, intestine; ooc, oocyte; oog, oogonia; ov, ovary.

victorellids (Braem, 1951) or nolellids (Calvet, 1900) as another example of species with highly elongated peristomes.

Numerous ctenostomes show a distinct muscular region in the cardia, which in some cases can form a highly muscular proventriculus or cardia (Markham & Ryland, 1987; Schwaha, 2020a). A simpler form is a mere cardiac constrictor that is found in all victorellids, where it is also genus-specific (Braem, 1951). For all ctenostomes, a distinct muscular cardia is absent in all alcyonidioideans, including the multiporate genera *Pherusella* (Decker et al., 2021), *Flustrellidra* and *Elzerina* (Schwaha, 2021). As the current study shows, a distinct muscular prominence of the cardiac region is missing, which furthermore shows a close resemblance to the remaining multiporate ctenostomes.

4.4 | Funicular system

An elaborate system of so-called funicular cords, peritoneal tissue strands that connect the polypide with the body wall, is typical for cheilostome bryozoans, but not so common for ctenostomes (Schwaha, Ostrovsky, et al., 2020). Many ctenostomes simply show one or two simple funicular muscles, whereas other taxa have a single proximal funiculus connecting the caecum to interzooidal pore plates as most typically found in vesicularioideans (e.g., Reed, 1988). Victorellid bryozoans show a similar proximal funicular strand with proximal branches extending to interzooidal pore plates. In *S. sibogae*, the funicular system is simpler and consists of a few cords extending from the gut to the interzooidal pore plates, which is similar to some other bryozoans (Schwaha, Ostrovsky, et al., 2020), including *Elzerina* (Schwaha, 2021). The extensive diffusely branching system of *S. floridensis* has multiple cords with some attaching to the body wall and others to the pore plates. Such complexity of the funicular system has not been described in any ctenostome. A similar system was construed to be present in *Lobiancopora* (Pergens, 1889), but this was not confirmed in more recent analyses (Hayward, 1985).

4.5 | Neuromuscular system

In the past decade, several studies were conducted on gymnolaemate bryozoans using immunocytochemical and confocal laser scanning microscopical methods (e.g., Decker et al., 2020; Prömer et al., 2021; Pröts et al., 2019; Schwaha & Wanninger, 2015; Schwaha et al., 2011; Temereva & Kosevich, 2016; Weber et al., 2014). The results are in accordance with previous descriptions of tubulinergic

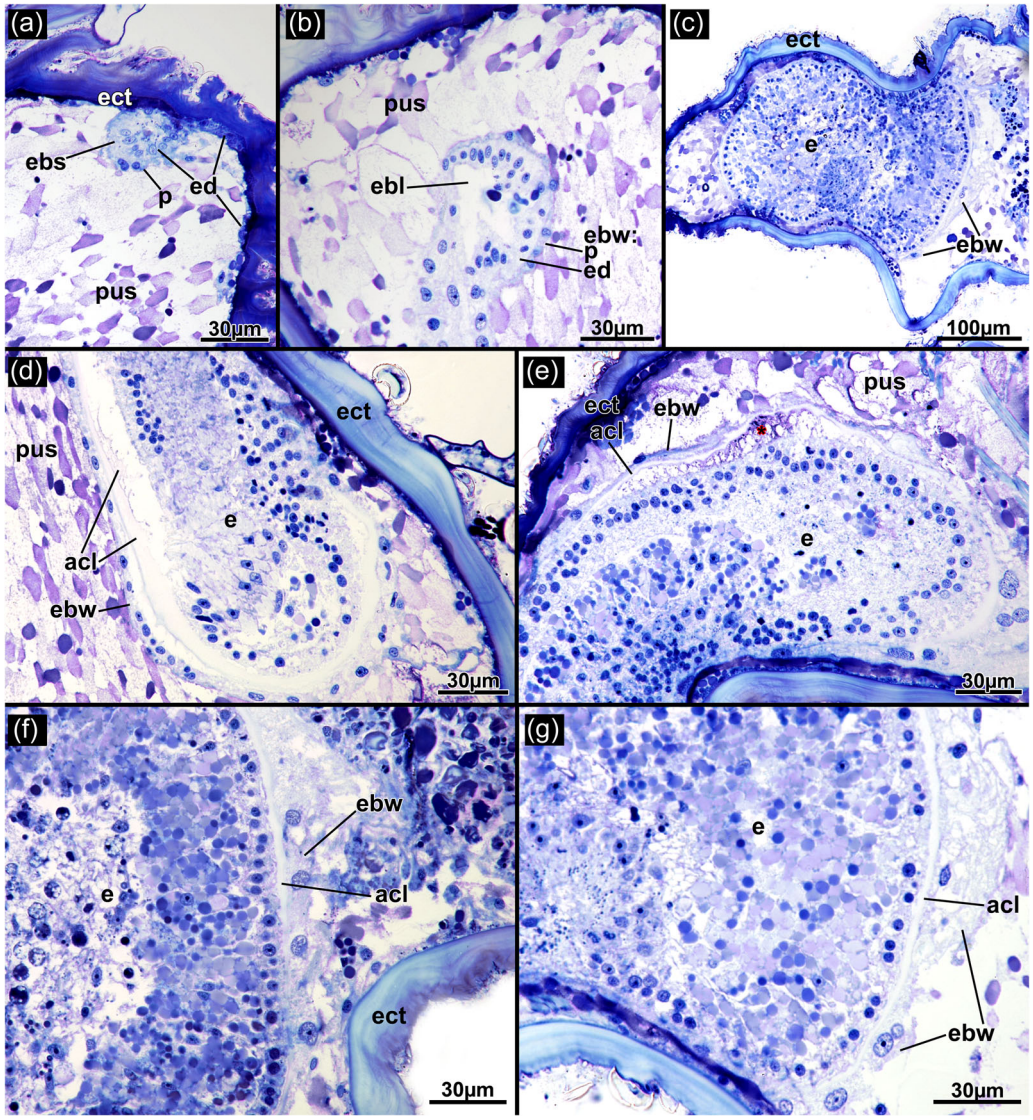

FIGURE 19 *Sundanella floridensis* sp. nov. Brooded embryo in an embryo sac of the body wall. (a) Attachment of the two-layered brood sac to the body wall. (b) Detail of the two layers of the embryo sac wall. (c) Overview of a brooded embryo within the embryo sac. (d) Detail showing an acellular secretion of the embryo sac internally towards the embryo. (e) Close association between embryo sac wall, embryo and the acellular secretions in between. (f, g) Details of the thickened embryo sac wall as opposed to the embryo. acl, acellular layer; e, embryo; ebl, embryo sac lumen; ebs, embryo sac; ebw, embryo sac wall; ect, ectocyst; ed, epidermis; p, peritoneum; pus, purple slabs within the body cavity.

immunocytochemical studies and show a concentration of neural tissue at the lophophoral base, mainly the cerebral ganglion and circum-oral nerve ring, from which most neurite bundles emanate. The highest resemblance of the sundanellid nervous system is with those of other gymnolaemates with high tentacle numbers as, for example, in pherusellids (Decker et al., 2020) or the cheilostome *Myriapora truncata* (Prömer et al., 2021). In general, there seems to be no distinct deviation from the general structure of the nervous system, except that no laterofrontal neurite bundles could be verified in the current study. However, given the limited availability for immunocytochemical studies, those neurite bundles might be present nonetheless.

The muscular system is similar to previous reports on ctenostome muscle systems (Schwaha & Wanninger, 2018) and has only a few notable details concerning the tentacle musculature. The frontal tentacle muscles are prominent in *Sundanella* and form a thick bundle, which has previously been recognized in *Flustrellidra hispida* (Shunatova & Tamberg, 2019). This seems to be a shared feature of these two genera.

4.6 | Reproduction in *Sundanella*

Previous observations on sundanellid development were conducted only by Braem on *S. sibogae* (1939). So far, our knowledge is incomplete and inconclusive: our data on *S. sibogae* show multiple early embryos embedded into the thinned vestibular wall, whereas previous observations found embryos immersed in

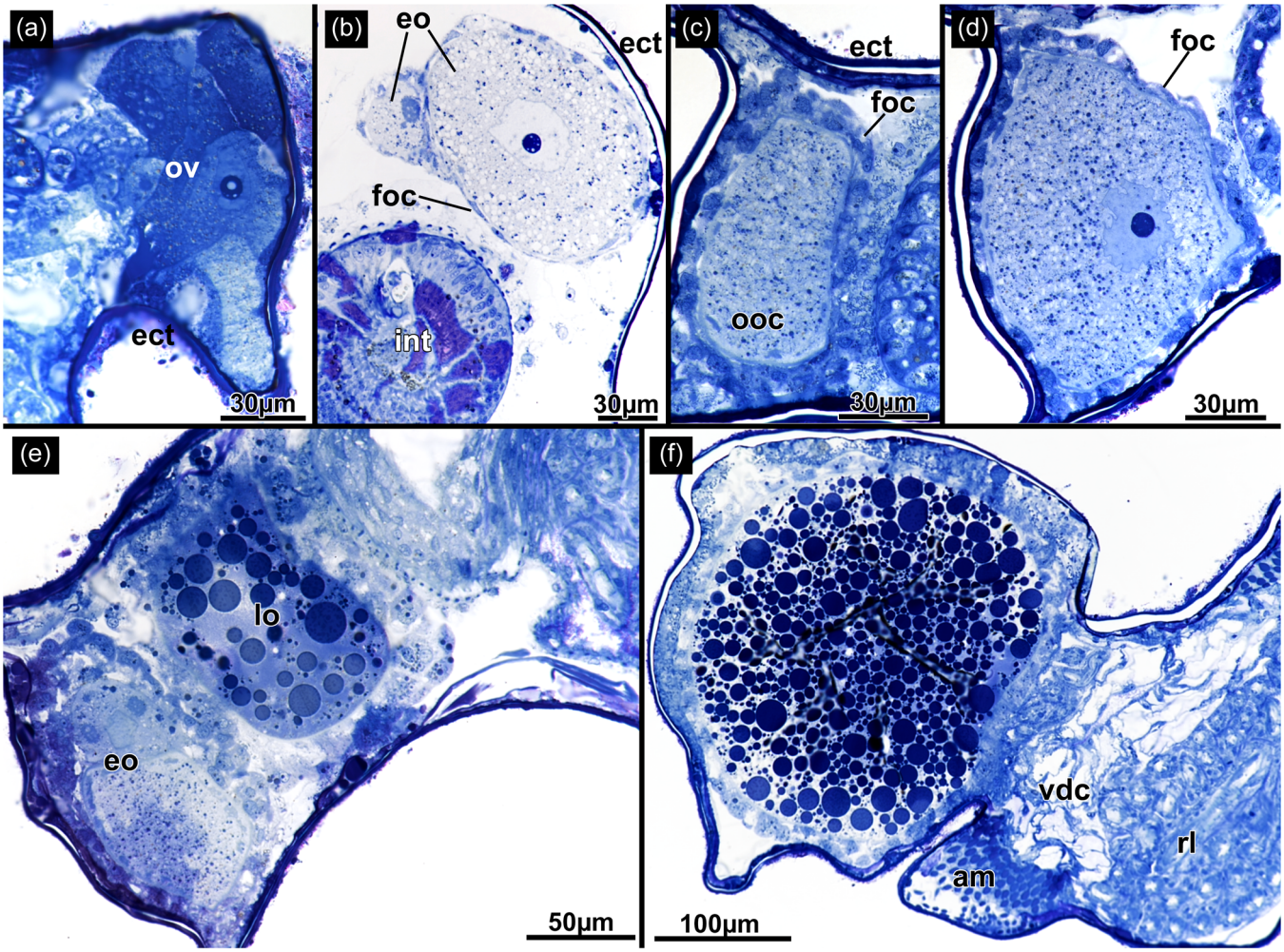

FIGURE 20 *Sundanella sibogae*. Reproductive aspects. Oogenesis. (a) Cluster of several early oocytes attached to the body wall. (b) Early oogenetic stages with a thin follicle epithelium. (c, d) Sections of later oocytes with thickened follicular epithelium. (e) Late oogenetic stage showing numerous large yolk inclusions. (f) Advanced oocyte with abundant yolk inclusions. am, apertural muscles; ect, ectocyst; eo, early oocyte; int, intestine; lo, late oocyte; ooc, oocyte; ov, ovary; rl, retracted lophophore; vdc, vacuolar diaphragmatic cells.

an invagination of the body wall forming a two-layered embryo sac with a rather hypertrophied epithelium (Braem, 1939). This is, in fact, a situation resembling phylactolaemate bryozoans (Bibermair et al., 2021; Ostrovsky et al., 2009, 2016). While the brooding of embryos in the vestibular wall is not uncommon (Ström, 1977), it often occurs in victorellid bryozoans (Braem, 1951). However, our results on the embryos of *S. floridensis* sp. nov. show that they were similarly embedded in a two-layered embryo sac as also previously found in *S. sibogae* (Braem, 1939). It is not entirely clear whether the deposition in the vestibular wall is transitory and embryos will later be transferred into an embryo sac of the body wall, but our results also coincide with the different oogenesis stages we encountered, that is, *S. sibogae* with vestibular wall-embedded embryos and more advanced to late oogenetic stages, whereas *S. floridensis* showed only the early beginning of oogenesis and an already large embryo embedded into embryo sacs. This could indicate that embryos are first embedded into the vestibular wall and perhaps later transferred into a pouch of the body wall, along with degeneration of the mother polypide. It is in any case doubtful why multiple larger oocytes are produced and first embedded in the vestibular wall when only one large embryo was encountered to be brooded in the body wall invagination of a single zooid.

It has previously been indicated that *Sundanella* is matrotrophic and nourishes its embryos during gestation (see Ostrovsky, 2020; Ostrovsky et al., 2009, 2016). While we have only limited material concerning embryonic growth, the structure of the embryo sac in *S. floridensis* clearly shows a hypertrophied epithelium that is surrounded by numerous intensely staining inclusions in the body cavity. Also, an acellular secretion seems evident towards the embryo in such late embryonic stages, which supports matrotrophy in this genus as recently also confirmed for another ctenostome (Schwaha, Ostrovsky, et al., 2020).

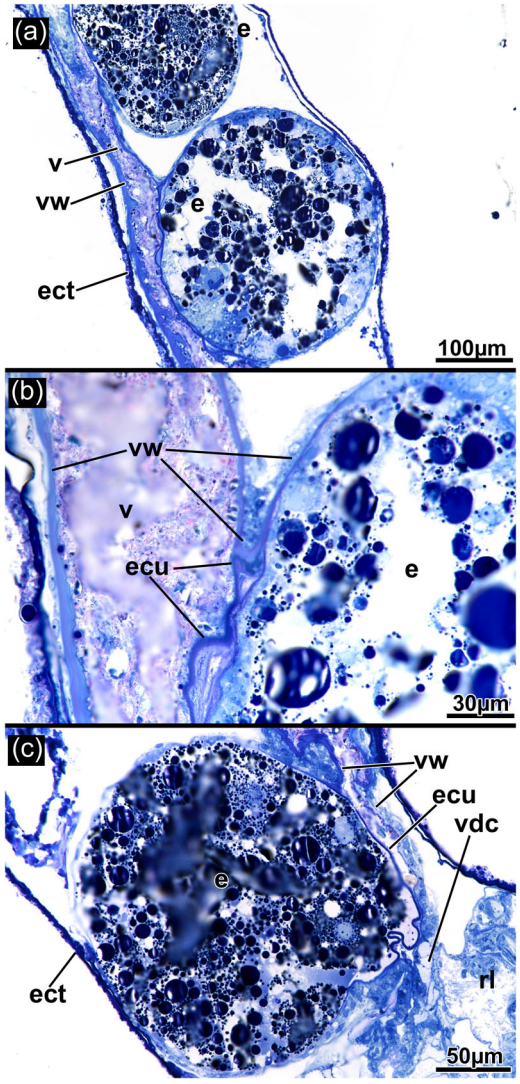

FIGURE 21 *Sundanella sibogae*, embryos brooded in pouches of the vestibular wall of a retracted zooid. (a) Two embryos embedded in the vestibular wall. (b) Detail showing the two different cuticles of the vestibular wall and the embryo. (c) Later embryo embedded in the vestibular wall. e, embryo; ect, ectocyst; ecu, cuticle of the embryo; rl, retracted lophophore; v, vestibulum; vdc, vacuolar diaphragmatic cells; vw, vestibular wall.

4.7 | The Multiporata concept

As demonstrated above, the genus *Sundanella* has little similarity or close relationship to victorellid ctenostomes as traditionally understood (e.g., d'Hondt, 1983). Instead, there are numerous characters relating it to other multiporate ctenostomes. These include the genera *Pherusella* (Decker et al., 2021) and flustrellidrid genera (Schwaha, 2021). Along with the pherusellids and flustrellidrids, *Sundanella* is the only ctenostome genus to have multiporate interzooidal pore plates, which is otherwise a common cheilostome character (Schwaha, Grischenko, et al., 2020). This supports the previous notion that multiporate interzooidal pore plates are an apomorphic character of a clade of alcyonidioidean ctenostomes that should be termed 'Multiporata' comprising Pherusellidae, Flustrellidrae and Sundanellidae. Supporting this close relationship are multiple morphological characters:

(1) high tentacle number of ~30 (contrary to the typical tentacle number of eight in victorellids);
(2) a bilateral lophophore with a rejection tract with two enlarged oral tentacles (see Decker et al., 2021; Schwaha, 2021);
(3) apertural muscles as a single large parietodiaphragmatic pair of muscles;
(4) frontal duplicature band with a broad basis ('king-size');
(5) collar vestibular (Schwaha, 2021);
(6) cuticle is often thick and multilayered, distinctly arborescent in certain areas (Schwaha, 2021; Schwaha, Grischenko, et al., 2020);
(7) funicular network sometimes quite elaborate;
(8) lack of muscular prominence in the cardia, a character shared with the remaining Alcyonidioidea (e.g., Alcyonidiidae, Clavoporidae).

Multiporate ctenostomes seem to reproduce mostly via brooding, as shown in all pherusellids (Decker et al., 2021), *Flustrellidra* (e.g., Kvach et al., 2019) and *Sundanella* (Braem, 1939, this study). Intertentacular organs as ovipositing structures are quite frequent in broadcasting species, but also occur in brooders (Ostrovsky & Porter, 2011). Among multiporates, an intertentacular organ has been found in *Haywardozoon* (Schwaha, Ostrovsky, et al., 2020), *Elzerina* (Schwaha, 2021) and *Sundanella* (this study). Generally, it is a transitory organ and could be more ubiquitous among multiporate ctenostomes, although it seems to be a feature that evolved multiple times independently (Ostrovsky & Porter, 2011).

It seems that there are three main configurations of interzooidal pore plates among ctenostome bryozoans (Figure 22).

Multiporates may have varying numbers of multiple communication pores in the interzooidal walls. Typically, the pores are rather small and the associated gymnolaemate-specific cell complex is of small size for each pore (Figure 22b). Such pore complexes always include the special cells that plug the pore and extend into each side of neighbouring zooids, the cincture cells that line the pore, being adjacent to the cystid wall and the limiting cells as a series of surrounding or covering cells in each pore (Figure 22). In the multiporate ctenostomes there usually seems to be only a single special cell associated with each pore (Decker et al., 2021; Schwaha, 2021).

The uniporate condition found in several other ctenostomes, such as *Arachnidium* (Schwaha & De Blauwe, 2020) or *Paludicella* (Schwaha, 2020b), generally exhibits a higher number of special cells, two to five, passing through each pore (Figure 22a,c). The most extreme example, with hypertrophy of pore-complex cells, is seen in hislopiid (Schwaha, 2020b) and vesicularioid ctenostomes (Bobin, 1964; Gordon, 1975) and includes multiple cells associated with each pore, the unimacroporate condition (Figure 22c). While these are all rather still superficial observations, it indicates that interzooidal pore

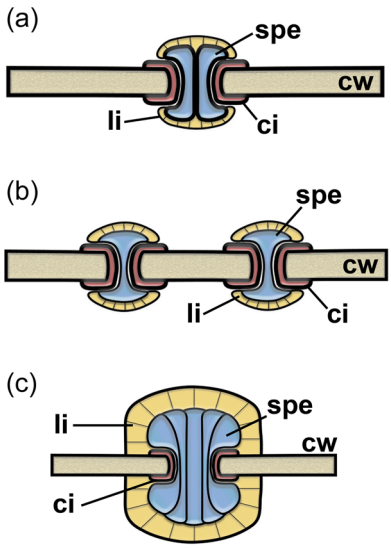

FIGURE 22 Schemes of interzooidal pore plate variation in ctenostome bryozoans. (a) Uniporate condition, (b) multiporate condition, (c) unimacroporate condition. ci, cincture cell; cw, cystid wall; li, limiting cell; spe, special cell.

structure shows multiple variations that merit further attention in the near future.

5 | CONCLUSIONS

This study confirms that soft-body morphology shows highly informative characters, not only for systematic and phylogenetic purposes but also for species discrimination. In fact, the high plasticity of cystid characters shown by our data as well from the literature demonstrates that proper species allocation is not possible without histological details. Also, all the evidence presented here confirms that sundanellid ctenostomes show only a superficial resemblance to victorellid ctenostomes. The general structure of the large, bilateral lophophore, the digestive tract with a vestibular anus and the entire apertural area, including its musculature and vestibular collar, confirm a close relationship to other multiporate ctenostomes, such as flustrellidrid or pherusellid ctenostomes.

ACKNOWLEDGEMENTS

Dennis P. Gordon gratefully acknowledges travel funding from the National University of Singapore in 2013 that enabled the collection and photography of *S. sibogae*. Recollection of material from Singapore in 2019 was funded by a grant to Dr Lee H. Liow (University of Oslo) by the European Research Council (ERC) under the European Union's Horizon 2020 research and innovation programme (grant agreement no. 724324 to Lee H. Liow). Laboratory processing and preservation at the National University of Singapore was supported by Dr Danwei Huang and Sudhanshi Jain. Judith E. Winston thanks the Smithsonian Marine Station for providing facilities for her research and Mary Spencer Jones, Natural History Museum, London, for her assistance with the examination of *Sundanella* specimens. Contribution no. 1179 from the Smithsonian Marine Station.

DATA AVAILABILITY STATEMENT

Data sharing not applicable to this article as no datasets were generated or analysed during the current study.

ORCID

Thomas Schwaha http://orcid.org/0000-0003-0526-6791

REFERENCES

Atkins, D. (1932). The ciliary feeding mechanism of the entoproct Polyzoa, and a comparison with that of the ectoproct Polyzoa. *Quarterly Journal of Microscopical Sciences*, *75*, 393–423.

Banta, W. C. (1975). Origin and early evolution of cheilostome Bryozoa. In S. Pouyet (Ed.), *Bryozoa 1974* (pp. 565–582). Université Claude Bernard.

Bibermair, J., Ostrovsky, A. N., Wanninger, A., & Schwaha, T. (2021). Reproductive biology, embryonic development and matrotrophy in the phylactolaemate bryozoan *Plumatella casmiana*. *Organisms Diversity & Evolution*, *21*, 467–490. https://doi.org/10.1007/s13127-021-00497-w

Bobin, G. (1964). Cytologie des rosettes de *Bowerbankia imbricata* (Adams) (Bryozoaire Cténostome, Vésicularine). Hypothèse sur leur fonctionnement. *Archives de Zoologie expérimentale et Générale*, *104*, 1–44.

Braem, F. (1939). *Victorella sibogae* Harm. *Zeitschrift für Morphologie und Ökologie der Tiere*, *36*, 267–278.

Braem, F. (1951). ÜBer *Victorella* und einige ihrer nächsten Verwandten, sowie über die Bryozoenfauna des Ryck bei Greifswald. *Zoologica*, *102*, 1–59.

Bros, W. E. (1987). Temporal variation in recruitment to a fouling community in Tampa Bay, Florida. *Journal of Coastal Research*, *3*, 499–504.

Calvet, L. (1900). Contribution à l'histoire naturelle des Bryozaires Ectoproctes marins. *Travaux de l'institut de Zoologie de l'Université de Montpellier et de la Station Zoologique de Cette N.S*, *8*, 1–488.

Cheetham, A. H., & Cook, P. L. (1983). General features of the class Gymnolaemata. In R. A. Robison (Ed.), *Treatise on invertebrate paleontology. Part G: Bryozoa* (pp. 138–207). Geological Society of America and University of Kansas.

Cook, P. L. (1968). Bryozoa (Polyzoa) from the coasts of tropical West Africa. *Atlantide Report*, *10*, 115–262.

Cook, P. L. (1985). Bryozoa from Ghana, a preliminary survey. *Koninklijk Museum voor Midden-Afrika. Zoologische Wetenshappen*, *238*, 1–315.

Decker, S., Gordon, D. P., Spencer Jones, M. E., & Schwaha, T. (2021). A revision of the ctenostome bryozoan family Pherusellidae, with description of two new species. *Journal of Zoological Systematics and Evolutionary Research*, *59*, 963–980.

Decker, S., Wanninger, A., & Schwaha, T. (2020). Morphology and life cycle of an epiphytic pherusellid ctenostome bryozoan from the Mediterranean Sea. *Organisms Diversity & Evolution*, *20*, 417–437. https://doi.org/10.1007/s13127-020-00443-2

d'Hondt, J. L. (1983). Tabular keys for identification of the recent ctenostomatous Bryozoa. *Mémoires de L'Institut Océanographique, Monaco*, *14*, 1–134.

Gordon, D. P. (1975). Ultrastructure of communication pore areas in two bryozoans. In S. Pouyet (Ed.), *Bryozoa 1974* (Vol. 3, pp. 187–192). Documents des Laboratoires de Géologie de la Faculté des Sciences de Lyon, hors sér.

Harmer, S. F. (1902). On the morphology of the Cheilostomata. *Quarterly Journal of Microscopical Sciences*, *46*, 263–350.

Harmer, S. F. (1915). The Polyzoa of the siboga expedition. Part 1. Entoprocta, ctenostomata and cyclostomata. *Siboga Expeditie*, *28A*, 1–180.

Hayward, P. J. (1985). Ctenostome Bryozoans, *Synopses of the British Fauna*. N. S. 33. E. J. Brill/Dr. W. Backhuys for The Linnean Society of London & The Estuarine and Brackish-Water Siences Association.

Jebram, D. (1973). Stolonen-entwicklung und systematik bei den Bryozoa ctenostomata. *Zeitschrift für zoologische Systematik und Evolutionsforschung*, *11*, 1–48.

Jebram, D. (1982). Interpretations of the results of feeding experiments regarding physiology, ecology, and phylogeny of the Bryozoa. *Zoologischer Anzeiger*, *208*, 405–416.

Kvach, A. Y., Varfolomeeva, M. A., Kotenko, O. N., Sukhotin, A. A., Kutiumov, V. A., Grischenko, A. V., Granovitch, A. I., & Ostrovsky, A. N. (2019). Life history of the ctenostome bryozoan *Flustrellidra hispida* in the White Sea. *Invertebrate Zoology*, *16*, 343–360.

Lutaud, G. (1964). Sur la structure et le rôle des glandes vestibulaires et sur la nature de certains organes de la cavité cystidiennce chez les Bryozaires Chilostomes. *Cahier de Biologie Marine*, *6*, 181–190.

Marcus, E. (1937). Briozoarios marinhos brasileiros I. *Boletim da Faculdade de filosofia, Ciências e Letras, Universidade di Sao Paolo, Zoologia*, *1*, 1–224.

Marcus, E. (1939). Bryozoarios marinhos brasileiros. III. *Boletim da Faculdade de Filosofia, Ciências e Letras, Universidade di Sao Paolo, Zoologia*, *3*, 111–353.

Marcus, E. (1941). Sobre Bryozoa do Brasil. I. *Boletim da Faculdade de Filosofia, Ciéncias e Letras, Universidade di Sao Paolo, Zoologia*, *5*, 3–208.

Markham, J. B., & Ryland, J. S. (1987). Function of the gizzard in Bryozoa. *Journal of Experimental Marine Biology and Ecology*, *107*, 21–37.

Martha, S. O., Vieira, L. M., Souto-Derungs, J., Grischenko, A. V., Gordon, D. P., & Ostrovsky, A. N. (2020). Gymnolaemata, Cheilostomata. In T. Schwaha (Ed.), *Handbook of zoology, phylum Bryozoa* (pp. 317–424). de Gruyter.

Matricon, I. (1960). Étude histologique d'*Alcyonidium polyoum* (Hassall) (Bryozoaire Cténostome). *Cahier de Biologie Marine*, *1*, 359–395.

Maturo, F. J. (1957). A study of the Bryozoa of Beaufort, North Carolina, and vicinity. *Journal of the Elisha Mitchell Scientific Society*, *73*, 11–68.

McKinney, F. K., & Dewel, R. A. (2002). The ctenostome collar—An enigmatic structure. In P. N. Wyse Jackson, C. J. Buttler, & M. E. Spencer-Jones (Eds.), *Bryozoan Studies 2001* (pp. 191–197). A.A. Balkema Publishers.

Mukai, H., Terakado, K., & Reed, C. G. (1997). Bryozoa. In F. W. Harrison & R. M. Woollacott (Eds.), *Microscopic anatomy of invertebrates* (Vol. 13, pp. 45–206). Wiley-Liss.

Osburn, R. C. (1940). Bryozoa of Porto Rico with a resume of West Indian Bryozoan fauna. *Scientific Survey of Porto Rico and the Virgin Islands*, *16*, 321–486.

Ostrovsky, A. N. (2020). Sexual reproduction in Bryozoa. In T. Schwaha (Ed.), *Handbook of zoology. Bryozoa* (pp. 101–122). de Gruyter.

Ostrovsky, A. N., Gordon, D. P., & Lidgard, S. (2009). Independent evolution of matrotrophy in the major classes of Bryozoa: Transitions among reproductive patterns and their ecological background. *Marine Ecology-Progress Series*, *378*, 113–124. https://doi.org/10.3354/meps07850

Ostrovsky, A. N., Lidgard, S., Gordon, D. P., Schwaha, T., Genikhovich, G., & Ereskovsky, A. V. (2016). Matrotrophy and placentation in invertebrates: A new paradigm. *Biological Reviews*, *91*, 673–711. https://doi.org/10.1111/brv.12189

Ostrovsky, A. N., & Porter, J. S. (2011). Pattern of occurrence of supraneural coelomopores and intertentacular organs in Gymnolaemata (Bryozoa) and its evolutionary implications. *Zoomorphology*, *130*, 1–15. https://doi.org/10.1007/s00435-011-0122-3

Pergens, E. (1889). Deux nouveaux types de bryozoaires cténostomes. *Annales de la Société Royale Malacologique de Belgique, Memoires*, *23*, 340–343.

Prömer, J., Sombke, A., & Schwaha, T. (2021). A comparative analysis of the nervous system of cheilostome bryozoans. *BMC Zoology*, *6*, 20. https://doi.org/10.1186/s40850-021-00084-8

Pröts, P., Wanninger, A., & Schwaha, T. (2019). Life in a tube: Morphology of the ctenostome bryozoan *Hypophorella expansa*. *Zoological Letters*, *5*, 28. https://doi.org/10.1186/s40851-019-0142-2

Prouho, H. (1892). Contribution à l'histoire des bryozaires. *Archives de Zoologie Expérimentale et Générale (2nd series)*, *10*, 557–656.

Reed, C. G. (1988). The reproductive biology of the gymnolaemate bryozoan *Bowerbankia gracilis* (Ctenostomata: Vesicularioidea). *Ophelia*, *29*, 1–23.

Ruthensteiner, B. (2008). Soft part 3D visualization by serial sectioning and computer reconstruction. *Zoosymposia*, *1*, 63–100.

Ryland, J. S. (1970). *Bryozoans*. Hutchinson University Library.

Santagata, S. (2008). The morphology and evolutionary significance of the ciliary fields and musculature among marine bryozoan larvae. *Journal of Morphology*, *269*, 349–364.

Schwaha, T. (2020a). Ctenostomata. In T. Schwaha (Ed.), *Handbook of zoology. Bryozoa* (pp. 269–316). de Gruyter.

Schwaha, T. (2020b). Morphology of bryozoans. In T. Schwaha (Ed.), *Handbook of zoology: Bryozoa* (pp. 57–100). de Gruyter.

Schwaha, T. (2020c). O anus, where art thou? An investigation of ctenostome bryozoans. *Journal of Morphology*, *281*, 914–922. https://doi.org/10.1002/jmor.21146

Schwaha, T. (2021). Morphology of ctenostome bryozoans. 3. *Elzerina*, *Flustrellidra*, *Bockiella*. *Journal of Morphology*, *282*, 633–651.

Schwaha, T., & De Blauwe, H. (2020). Morphology of ctenostome bryozoans: 1 Arachnidium fibrosum. *Journal of Morphology*, *281*, 1598–1606. https://doi.org/10.1002/jmor.21275

Schwaha, T., Grischenko, A. V., & Melnik, V. P. (2020). Morphology of ctenostome bryozoans: 2. *Haywardozoon pacificum*, with implications of the phylogenetic position of the genus. *Journal of Morphology*, *281*, 1607–1616. https://doi.org/10.1002/jmor.21272

Schwaha, T., Grischenko, A. V., & Melnik, V. P. (2021). Morphology of ctenostome bryozoans: 4 *Pierrella plicata*. *Journal of Morphology*, *282*, 746–753. https://doi.org/10.1002/jmor.21344

Schwaha, T., Ostrovsky, A. N., & Wanninger, A. (2020). Key novelties in the evolution of aquatic colonial phylum Bryozoa: Evidence from soft body morphology. *Biological Reviews*, *95*, 696–729.

Schwaha, T., & Wanninger, A. (2018). Unity in diversity: A survey of muscular systems of ctenostome Gymnolaemata (Lophotrochozoa, Bryozoa). *Frontiers in Zoology*, *15*, 24.

Schwaha, T., Wood, T. S., & Wanninger, A. (2011). Myoanatomy and serotonergic nervous system of the ctenostome *Hislopia malayensis*: Evolutionary trends in bodyplan patterning of ectoprocta. *Frontiers in Zoology*, *8*, 11.

Schwaha, T. F., & Wanninger, A. (2015). The serotonin-lir nervous system of the Bryozoa (Lophotrochozoa): A general pattern in the Gymnolaemata and implications for lophophore evolution of the phylum. *BMC Evolutionary Biology*, *15*, 223. https://doi.org/10.1186/s12862-015-0508-9

Shier, D. E. (1964). Marine Bryozoa from northwest Florida. *Bulletin of Marine Science*, *14*, 603–662.

Shunatova, N., & Tamberg, Y. (2019). Body cavities in bryozoans: Functional and phylogenetic implications. *Journal of Morphology*, *280*, 1332–1358. https://doi.org/10.1002/jmor.21034

Silbermann, S. (1906). Untersuchungen über den feineren Bau von *Alcyonidium mytili*. *Archiv für Naturgeschichte*, *72*, 1–78.

Ström, R. (1977). Brooding patterns of bryozoans. In R. M. Woollacott & R. L. Zimmer (Eds.), *Biology of bryozoans* (pp. 23–55). Academic Press.

Taylor, P. D., & Waeschenbach, A. (2015). Phylogeny and diversification of bryozoans. *Palaeontology*, *58*, 585–599. https://doi.org/10.1111/pala.12170

Temereva, E. N., & Kosevich, I. A. (2016). The nervous system of the lophophore in the ctenostome *Amathia gracilis* provides insight into the morphology of ancestral ectoprocts and the monophyly of the lophophorates. *BMC Evolutionary Biology*, *16*, 181. https://doi.org/10.1186/s12862-016-0744-7

Todd, J. A. (2000). The central role of ctenostomes in bryozoan phylogeny. In A. Herrera Cubilla & J. B. C. Jackson (Eds.), *Proceedings of the 11th International Bryozoology Association Conference* (pp. 104–135). Balboa, Panama: Smithsonian Tropical Research Institute.

Vieira, L. M., Migotto, A. E., & Winston, J. E. (2014). Ctenostomatous Bryozoa from Sao Paulo, Brazil, with descriptions of twelve new species. *Zootaxa*, *3889*, 485–524.

Waeschenbach, A., Cox, C. J., Littlewood, D. T. J., Porter, J. S., & Taylor, P. D. (2009). First molecular estimate of cyclostome bryozoan phylogeny confirms extensive homoplasy among skeletal characters used in traditional taxonomy. *Molecular Phylogenetics and Evolution*, *52*, 241–251. https://doi.org/10.1016/j.ympev.2009.02.002

Waters, A. W. (1894). Observations on the gland-like bodies in the Bryozoa. *Journal of the Linnean Society, Zoology*, *24*, 272–278.

Weber, A., Wanninger, A., & Schwaha, T. (2014). The nervous system of *Paludicella articulata*—First evidence of a neuroepithelium in a ctenostome ectoproct. *Frontiers in Zoology*, *11*, 89.

Winston, J. E. (1982). Marine bryozoans (Ectoprocta) of the Indian River area (Florida). *Bulletin of the American Museum of Natural History*, *173*, 99–176.

SUPPORTING INFORMATION

Additional supporting information can be found online in the Supporting Information section at the end of this article.

How to cite this article: Schwaha, T., Winston, J. E., & Gordon, D. P. (2022). Morphology of ctenostome bryozoans: 5. *Sundanella*, with description of a new species from the Western Atlantic and the Multiporata concept. *Journal of Morphology*, 283(9), 1139–1162. https://doi.org/10.1002/jmor.21494